



Title	Coxsackie and adenovirus receptor (CAR) is a product of Sertoli and germ cells in rat testes which is localized at the Sertoli-Sertoli and Sertoli-germ cell interface
Author(s)	Wang, CQF; Mruk, DD; Lee, WWM; Cheng, CY
Citation	Experimental Cell Research, 2007, v. 313 n. 7, p. 1373-1392
Issued Date	2007
URL	http://hdl.handle.net/10722/48723
Rights	Creative Commons: Attribution 3.0 Hong Kong License

available at www.sciencedirect.comwww.elsevier.com/locate/yexcr

Research Article

Coxsackie and adenovirus receptor (CAR) is a product of Sertoli and germ cells in rat testes which is localized at the Sertoli–Sertoli and Sertoli–germ cell interface

Claire Q.F. Wang^a, Dolores D. Mruk^a, Will M. Lee^b, C. Yan Cheng^{a,*}

^aCenter for Biomedical Research, The Population Council, 1230 York Avenue, New York, NY 10021, USA

^bDepartment of Zoology, University of Hong Kong, Hong Kong, China

ARTICLE INFORMATION

Article Chronology:

Received 30 August 2006

Revised version received

26 December 2006

Accepted 23 January 2007

Keywords:

Testis

Spermatogenesis

Sertoli-germ cell interaction

Blood–testis barrier

Tight junction

Adherens junction

Ectoplasmic specialization

ABSTRACT

The coxsackie and adenovirus receptor (CAR), a putative cell–cell adhesion molecule, has attracted wide interest due to its importance in viral pathogenesis and in mediating adenoviral gene delivery. However, the distribution pattern and physiological function of CAR in the testis is still not clear. Here, we identified CAR in Sertoli cells and germ cells of rats. *In vivo* studies have shown that CAR resides at the blood–testis barrier as well as at the ectoplasmic specialization. The persistent expression of CAR in rat testes from neonatal period throughout adulthood implicates its role in spermatogenesis. Using primary Sertoli cell cultures, we observed a significant induction of CAR during the formation of Sertoli cell epithelium. Furthermore, CAR was seen to be concentrated at inter-Sertoli cell junctions, co-localizing with tight junction protein marker ZO-1 and adherens junction protein N-cadherin. CAR was also found to be associated with proteins of Src kinase family and its protein level declined after TNF α treatment in Sertoli cell cultures. Immunofluorescent staining of isolated germ cells has revealed the presence of CAR on spermatogonia, spermatocytes, round spermatids and elongate spermatids. Taken together, we propose that CAR functions as an adhesion molecule in maintaining the inter-Sertoli cell junctions at the basal compartment of the seminiferous epithelium. In addition, CAR may confer adhesion between Sertoli and germ cells at the Sertoli–germ cell interface. It is possible that the receptor utilized by viral pathogens to breakthrough the epithelial barrier was also employed by developing germ cells to migrate through the inter-Sertoli cell junctions.

© 2007 Published by Elsevier Inc.

Introduction

CAR is a 46-kDa transmembrane protein that enables viral attachment and entry into cells for coxsackie virus group B and adenovirus groups 2 and 5 [1]. The availability of CAR on

cell surface is a determining factor of a cell's susceptibility to adenoviral vectors for gene delivery [2]. Therefore, extensive studies have been carried out to establish the expression profile of CAR in a variety of human tissues that are of interest to gene therapy, such as brain, heart and muscles [3–6].

* Corresponding author. Fax: +1 212 327 8733.

E-mail address: Y-Cheng@popcbr.rockefeller.edu (C.Y. Cheng).

59 As a structural component of tight junction and/or ad-
60 herens junction, CAR is engaged in homotypical trans-inter-
61 action at regions of cell-cell contact, promoting cell adhesion
62 and tissue genesis [6-8]. It has been found to associate with
63 scaffolding proteins ZO-1 and β -catenin [8,9]. With two
64 immunoglobulin-like domains in the extracellular region, a
65 single transmembrane domain and a cytoplasmic tail [1,10],
66 CAR joins JAMs and nectins to become a member of the
67 immunoglobulin (Ig) superfamily. Integral transmembrane
68 proteins of Ig superfamily are implicated in cell adhesion
69 and migration. For example, JAM-C was described to promote
70 neutrophil trans-endothelial migration [11], whereas nectin-
71 like molecule-5 has been shown to enhance cell movement in
72 NIH3T3 cells [12].

73 In adult rat testes, preleptotene spermatocytes traverse
74 the blood-testis barrier from the basal to the adluminal
75 compartment of the seminiferous epithelium for further
76 development [13]. While they migrate progressively towards
77 the lumen, spermatocytes differentiate into round and
78 elongate spermatids until they detach from the epithelium
79 at stage VIII of the epithelial cycle at spermatogenesis [13].
80 This movement of germ cells involves rapid disassembly and
81 reassembly of Sertoli-Sertoli and Sertoli-germ cell junctions
82 [14]. Transmembrane proteins at the Sertoli-germ cell inter-
83 face, for example, cadherins, nectins, integrins and JAMs,
84 function as anchoring devices to maintain attachment
85 between the two types of cells. More importantly, these
86 proteins work in concert to facilitate the movement of germ
87 cells [15]. To date, knockout studies of nectin-2 and JAM-C
88 have yielded mice that were defective in spermatogenesis
89 [16,17], illustrating the essential roles of these adhesion
90 molecules in spermatogenesis.

91 Due to the structural similarity between CAR, JAMs and
92 nectins, we aimed to investigate the presence of CAR in
93 different cell types of the testis and its physiological sig-
94 nificance to spermatogenesis. A recently published study has
95 identified CAR at the acrosome region of mouse and human
96 spermatozoa, as well as its interaction with JAM-C [18].
97 However, the presence of CAR at the Sertoli-Sertoli cell
98 interface or tight junctions at the blood-testis barrier is not
99 clear, nor do we know for certain about its expression in germ
100 cells during their differentiation in the testis. In this report, we
101 carried out *in vivo* and *in vitro* experiments to examine the
102 cellular localization of CAR in Sertoli and developing germ
103 cells, as well as its expression pattern during testicular
104 maturation. In addition, we studied the interaction of CAR
105 with peripheral regulatory proteins and the effects of cyto-
106 kines treatment (e.g. TNF α) on its expression level in primary
107 Sertoli cell cultures. These data will help elucidate the
108 physiological role of CAR as a cell adhesion protein in
109 spermatogenesis.

Materials and methods 110

Animals 112

113 Male Sprague-Dawley rats were obtained from Charles River
114 Laboratories (Kingston, NY). Rats were sacrificed by CO₂
115 asphyxiation. The use of animals for this study was approved
116 by the Rockefeller University Animal Care and Use Committee
117 with Protocol Numbers 00111, 03017 and 06018.

RT-PCR 118

119 Total RNA was extracted from tissues or cells by Trizol
120 Reagent (Invitrogen). About 2 μ g of total RNA was reverse
121 transcribed into cDNAs using 0.3 μ g of oligo(dT)₁₅ with a
122 Moloney murine leukemia virus reverse transcription kit
123 (Promega) in a final reaction volume of 25 μ L. PCR reaction
124 mixture was composed of 2-3 μ L of RT product, with 0.4 μ g of
125 both the sense and anti-sense primers targeted to CAR (see
126 Table 1). Co-amplification of rat ribosomal S16 gene was
127 included to ensure the quality of RT product and the correct
128 composition of each reaction mixture. The cycling parameters
129 used in amplifying CAR are as follows: denaturation at 94 $^{\circ}$ C
130 for 1 min, annealing at 58-59 $^{\circ}$ C for 1 min, and extension at
131 72 $^{\circ}$ C for 1.5 min, for a total of 26 cycles. After the reaction,
132 10 μ L aliquots of PCR product were resolved by 5% T
133 polyacrylamide gels using 0.5 \times TBE (45 mM Tris-borate,
134 1 mM EDTA, pH 8.0) as a running buffer.

Antibodies 135

136 Primary antibodies purchased from different vendors are listed
137 in Table 2. Each antibody used in this study was shown to
138 cross-react with its corresponding rat protein in our prelimin-
139 ary experiments. Bovine anti-rabbit IgG, bovine anti-goat IgG
140 and goat anti-mouse IgG conjugated to horseradish peroxidase
141 were purchased from Santa Cruz Biotechnology. The rabbit
142 anti-CAR (H300) polyclonal antibody used in this study was
143 raised against amino acid residues 1-300 mapping the N-
144 terminus of CAR from human origin, which cross-reacted with
145 the rat protein as indicated by the manufacturer. The two
146 predominant isoforms of CAR differ only at the extreme C-
147 terminus of the intracellular tail [10,19,20], therefore the anti-
148 CAR (H-300) IgG detected both variants of this protein.

Primary testicular cell cultures 149

Sertoli cells 150

151 Sertoli cells were isolated from 20-day-old rats as previously
152 described [21]. Freshly isolated cells were cultured at high cell

t1.1 **Table 1 – Primers for RT-PCR analysis of CAR and S16**

t1.2 Gene	t1.3 Primer sequence	Orientation	Position	Length (bp)	Reference
t1.4 CAR	5'-GGAAACTGCCTATCTACCCTGCAA-3'	Sense	173-196	531	GenBank Accession
t1.5	5'-CTGTAGGTCCCAGAATACTCAGAACT-3'	Anti-sense	678-703		Number: NM-053570
t1.6 S-16	5'-TCCGCTGCAGTCCGTTCAAGTCTT-3'	Sense	15-38	385	[51]
t1.7	5'-GCCAAACTTCTTGGATTGCGAGCG-3'	Anti-sense	376-399		

Table 2 – Sources of antibodies and their working dilutions used for different experiments in this report

Vendor	Antibody against target protein ^a	Animal source	Catalog no.	Lot no.	Use ^b	Working dilution ^c											
Santa Cruz Biotechnologies (Santa Cruz, CA)	CAR	Rabbit	sc-15405	J1304	IP												
					IB	1:200											
					IF	1:50											
	CAR	Goat	sc-10313	F0304	IHC	1:100											
						Mouse, monoclonal	sc-32795	E2605	IB	1:200							
							Occludin	Rabbit	sc-5562	G2803	IB	1:200					
						JAM-C	Goat	sc-23005	L1704	IF	1:50						
						Actin	Goat	sc-1616	J0104	IB	1:200						
						CAR	Goat	sc-10313	F0304	IP							
						α -Catenin	Rabbit	sc-7894	A2705	IP							
						β -Catenin	Rabbit	sc-7199	F0204	IP							
						γ -Catenin	Rabbit	sc-7900	J139	IP							
						Vinculin	Rabbit	sc-5573	I 2204	IP							
						α -Actinin	Goat	sc-7453	D292	IP							
						FAK	Rabbit	sc-558	D1806	IP							
						c-Src	Mouse, monoclonal	sc-8056	F3006	IF	1:100						
						Upstate Biotechnology (Lake Placid, NY)	PI-3kinase	Rabbit	06497	25006	IP						
												p130 cas	Rabbit	06500	19950	IP	
												Src, CT, clone NL19	Rabbit, Monoclonal	05-772	26812	IP	
BD Biosciences (San Jose, CA)	Integrin β 1	Mouse, monoclonal	610468	53855	IP	1:1000											
						Espin	Mouse, monoclonal	611656	32291	IF	1:100						
Zymed Laboratories Inc. (South San Francisco, CA)	N-Cadherin	Mouse, monoclonal	33-3900	50393487	IF	1:50											
						ZO-1 FITC conjugate	Mouse, monoclonal	33-91111	60102882	IF	1:50						
	JAM-A	Rabbit	36-1700	40890360	IB	1:200											
	Goat anti-mouse FITC conjugate	Goat	81-6511	40397219	IF	1:50											
	Goat anti-rabbit Cy3 conjugate	Goat	81-6115	51001169	IF	1:50											
Chemicon (Temecula, CA)	Donkey anti-mouse FITC conjugate	Donkey	AP192F	508006630	IF	1:100											
						Donkey anti-rabbit Cy3 conjugate	Donkey	AP182C	24010618	IF	1:100						
						Donkey anti-goat FITC conjugate	Donkey	AP180F	24011222	IF	1:100						

^a All primary antibodies used in this report were polyclonal antibodies unless otherwise specified. It is noted that all antibodies obtained commercially cross-reacted with the corresponding rat proteins.

^b IB: immunoblotting; IF, immunofluorescent microscopy; IHC, immunohistochemistry; IP, immunoprecipitation.

^c Working dilution of primary antibodies was prepared in ~30 ml of PBS–Tris. For all IP experiments, 2 μ g IgG for each antibody against its corresponding target protein was used per reaction tube.

density (0.5×10^6 cells/cm²) on Matrigel (BD Biosciences)-coated 12-well dishes (effective surface area, 3.83 cm² per well; containing 3 mL medium, with $\sim 2 \times 10^6$ Sertoli cells). Serum-free Ham's F12 nutrient mixture and Dulbecco's modified Eagle's medium (F12/DMEM, 1:1, vol./vol.) was supplemented with gentamicin (20 mg/L), 15 mM HEPES, sodium bicarbonate (1.2 g/L), bovine insulin (10 μ g/mL), human transferrin (5 μ g/mL), epidermal growth factor (2.5 ng/mL) and bacitracin (5 μ g/mL). Cultures were designated as "time 0" at the time of plating. Cells were then incubated at 35 °C in a humidified atmosphere of 95% air–5% CO₂. To obtain Sertoli cell cultures with purity greater than 98%, cells were hypotonically treated 36 h after plating with 20 mM Tris (pH 7.4), for 2.5 min at 22 °C to lyse contaminating germ cells [22]. The wells were then washed twice with F12/DMEM, media were replaced every 24 h, and cells were incubated for an additional 5–7 days [23], however, it is noted that functional tight and anchoring junctions were established within 2–3 days after cell plating (see below) [23]. To terminate cultures at specified time points, cells were rinsed with cold PBS once and then scraped from the wells with lysis buffer for protein lysate preparation. For immunofluorescent staining, Sertoli

cells were cultured at low density (0.1×10^6 cells/cm²) to allow the formation of a confluent monolayer with tight junction and anchoring junctions. Cells plated at higher densities often grow into an epithelium with overlapping cell layers, which would later become an obstacle for imaging cell borders.

Germ cells

Germ cells were isolated from 90-day-old rats by a mechanical procedure without the use of trypsin as previously described [24]. Since the glass wool filtration step was omitted from the isolation procedures, germ cell preparation for this study contained elongating/elongated spermatids. The ratio of spermatogonia:spermatocytes:round spermatids:elongating/elongate spermatids was similar to that of germ cells *in vivo* when assessed by DNA flow cytometry [24]. Germ cells were used immediately after isolation.

Sertoli cells and germ cells isolated with the above described protocol contained negligible contamination of other type of cells, which was verified by RT-PCR and immunoblotting analysis of cell-type specific protein markers [25]. For example, c-kit receptor was amplified by RT-

196 PCR and probed in immunoblot to detect possible germ cell
197 contamination. Likewise, testin, 3β -hydrosteroid dehydro-
198 genase, and fibronectin were used to monitor the presence
199 of contaminating Sertoli cells, Leydig cells and peritubular
200 myoid cells, respectively [25].

201 *Transepithelial electrical resistance (TER)*

202 The establishment of tight junction permeability barrier was
203 assessed by quantifying the TER across the cell epithelium as

204 described [26]. In brief, Sertoli cells were isolated from 20-day-
205 old rats and seeded at a cell density of 0.75×10^6 cells/cm². Such
206 density is required for TER studies, because low-density cell
207 cultures would generate small blank areas with no or very few
208 cells on the bicameral units, forming leaky spots for electric
209 current to pass through. This renders TER measurement
210 inaccurate or impossible. Cells were plated onto the bicameral
211 units with F12/DMEM medium in each of the apical and basal
212 chambers. The assembly of inter-Sertoli tight junctions was
213 assessed by TER across the Sertoli cell epithelia using a

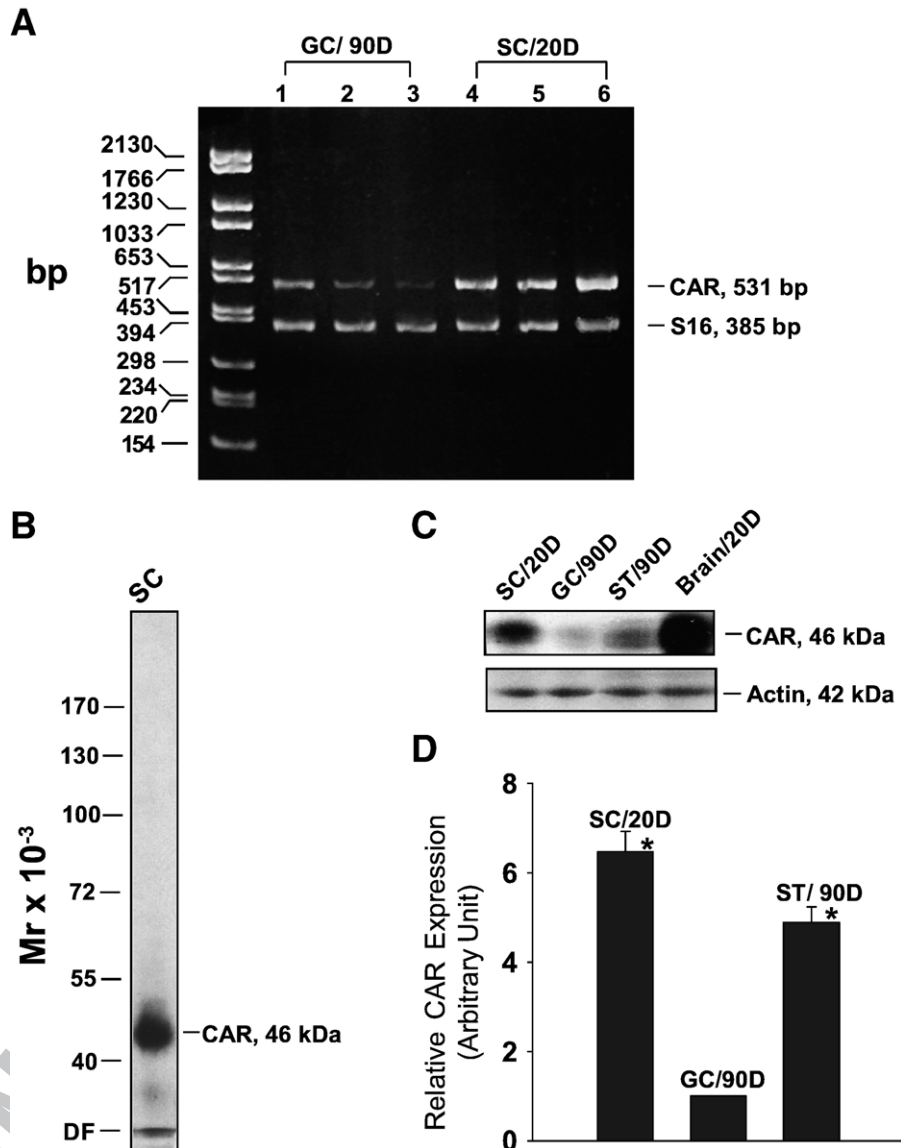


Fig. 1 – Expression of CAR in Sertoli and germ cells. (A) Results of RT-PCR using total RNA isolated from Sertoli (SC) and germ cells (GC) to assess the steady-state mRNA level of CAR. DNA size marker is on the left (bp, base pair). Each lane represents Sertoli cell or germ cell RNA extracted from a separate batch of cells. D, day. (B) A single prominent band corresponding to the apparent Mr of CAR at 46 kDa was detected on the immunoblot using Sertoli cell lysate (100 μ g protein), illustrating the specificity of this antibody. DF, dye-front. (C) Protein extracts of Sertoli cells (from 20-day-old rats), germ cells (from 90-day-old rats) and seminiferous tubules (from 90-day-old rats) were analyzed by immunoblotting, using a rabbit anti-CAR (H-300, Santa Cruz) polyclonal antibody. The same blot was probed with β -actin to confirm equal protein loading. Protein lysate of rat brain (from 20-day-old rats) was loaded onto the same gel, serving as positive control. D, day. (D) Bar graph summarizes results of three sets of immunoblots using different batches of lysates from Sertoli and germ cells and seminiferous tubules (ST). D, day. The level of CAR in germ cells was arbitrarily set at 1 against which 1-way ANOVA was performed. * $P < 0.01$.

214 Millicell (Millipore Corp) electrical resistance system. Briefly,
 215 current was passed through the epithelial monolayer between
 216 two silver-silver chloride electrodes. Resistance was calcu-
 217 lated from the change in ohm (Ω) across the monolayer

218 induced by a short (~ 2 s) 20- μ A pulse of current. The
 219 resistance was multiplied by the surface area of the filter to
 220 yield the area resistance in Ω cm^2 . The net value of electrical
 221 resistance was then computed by subtracting the background,

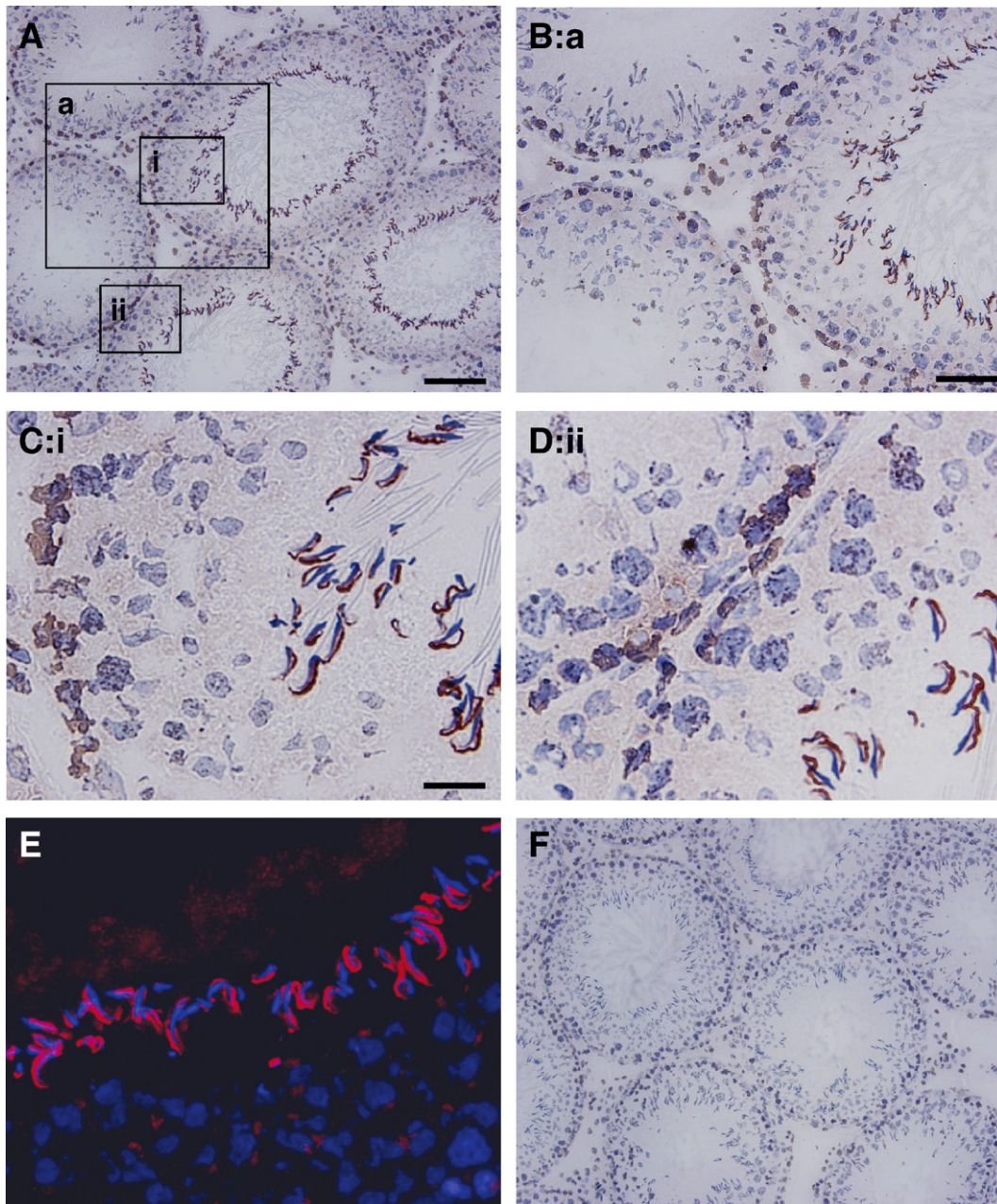


Fig. 2 – Localization of CAR in the seminiferous epithelium of adult rat testes by immunohistochemistry. (A) Frozen sections of adult rat testes were stained using a rabbit anti-CAR polyclonal antibody. Signal was detected at the basal compartment of the epithelium in virtually all stages of the epithelial cycle. However, strongest staining was found at the apical ectoplasmic specialization in stage VIII tubules. (B) Magnified view of the boxed area “a” in A, showing CAR staining at the basal compartment, which is consistent with its localization at the blood–testis barrier. (C–D) Corresponding to boxed area (i) and (ii). Sickle-shaped CAR staining was concentrated at site of apical ES in stage VIII seminiferous tubules, where elongated spermatids anchor onto Sertoli cells in the epithelium. CAR staining was also found at the site of blood–testis barrier. (E) Localization of CAR by immunofluorescent staining. Sections were incubated with a rabbit anti-CAR, to be followed by a donkey anti-rabbit IgG–Cy3 conjugate. Cell nuclei were visualized by DAPI staining. Merged image of CAR and DAPI staining identified CAR at the apical and round spermatids. (F) Control experiment in which testis sections were stained with normal rabbit IgG at the same dilution as the primary antibody shown in A–E. Scale bar = 100 μm in A, which also applies to F. Scale bar = 50 μm in B. Scale bar = 15 μm in C, which also applies to D and E.

222 which was measured on Matrigel-coated cell-free bicameral
223 units, from values of Sertoli cell-plated chambers [26]. Under
224 these conditions, inter-Sertoli tight junctions were mostly
225 formed at ~2–3 days [23]. Each time point had triplicate
226 cultures, and each experiment was repeated 3 times using
227 different batches of primary Sertoli cell cultures.

228 Immunofluorescent microscopy

229 Frozen cross sections of testes (~6 μm) obtained in a cryostat
230 were mounted on poly-L-lysine-coated slides, fixed with
231 Bouin's fixative and permeabilized with 0.2% Triton X-100
232 for 5 min. Sections are then washed with PBS and blocked with
233 10% normal goat or donkey serum for 1 h. This is followed by
234 incubation with primary antibodies overnight at room tem-
235 perature (see Table 2 for working dilutions). Slides were
236 washed in PBS before incubation with secondary antibodies
237 conjugated with FITC (green) or Cy3 (red). Sections were
238 mounted in Vectashield Hardset with 4',6'-diamino-2-phenyl-
239 indole (DAPI) (Vector Laboratories, Burlingame, CA). Fluores-
240 cent micrographs were acquired by using an Olympus BX40
241 microscope (Olympus Corp., Melville, NY) equipped with
242 Olympus UPlanF1 fluorescent optics and an Olympus DP70
243 12.5 MPa digital camera. Sections were also stained with
244 normal rabbit, mouse or goat IgG as negative controls. For cell
245 staining, Sertoli cells were cultured for 2 to 3 days at
246 0.1×10^6 cells/cm² on Lab-Tek® Chamber Slide™ Systems
247 (Nalgene Nunc International) before fixation with Bouin's
248 solution and immunofluorescent microscopy was performed
249 as detailed above. To eliminate inter-experimental variations,
250 all samples within an experimental group were processed
251 simultaneously by mounting 2–3 cross sections per slide.
252 Several slides were processed in parallel. Immunohistochem-
253 istry studies were handled with the same practice.

254 Immunohistochemistry

255 Immunohistochemistry was performed with a Histostain-SP™
256 kit (Zymed, CA). Frozen sections of (~6 μm) of testes were

257 mounted onto poly-L-lysine-coated slides and fixed in Bouin's
258 fixative. Sections were treated with 3% H₂O₂ in methanol (vol./
259 vol.) to block the endogenous peroxidase activity, to be
260 followed by incubation with 10% normal goat serum to block
261 nonspecific binding. Thereafter, sections were incubated with
262 a rabbit-anti-CAR (Santa Cruz, CA; dilution 1:100) polyclonal
263 antibody in a moist chamber at room temperature overnight.
264 Sections were then incubated in biotinylated secondary anti-
265 body for 30 min and treated with streptavidin peroxidase for
266 approximately 5 min. Immunoreactive CAR appeared as
267 reddish-brown precipitates on the sections. Slides were then
268 counterstained with hematoxylin and mounted in glycerol
269 vinyl alcohol (GVA, Zymed). Negative controls were included
270 by incubating the sections with normal rabbit IgG at the same
271 dilution as the primary antibody. Micrographs reported herein
272 were representative results from 3 to 6 experiments using
273 different samples.

Immunoblot analysis

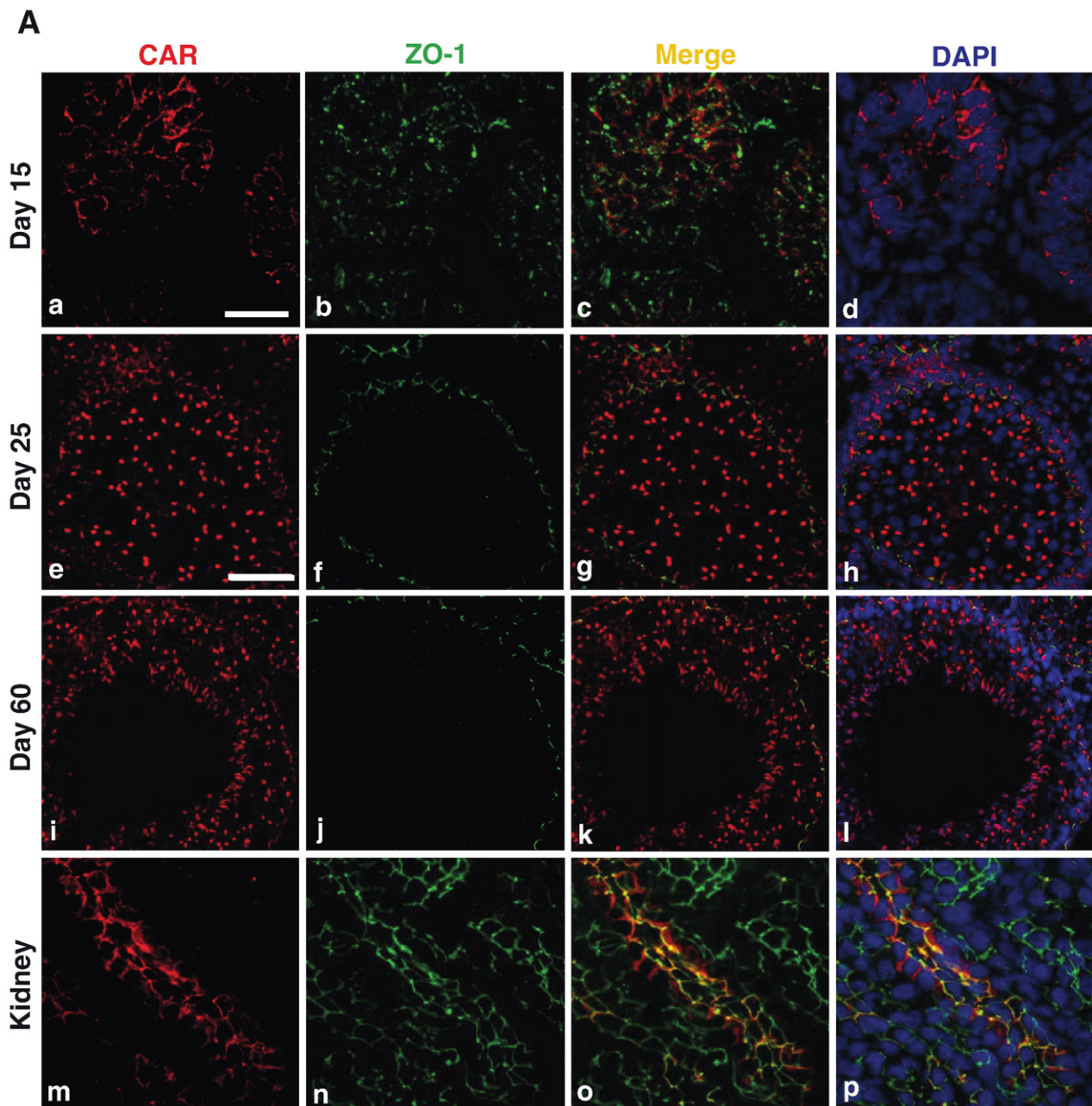
274
275 Testes or cell lysates were prepared in immunoprecipitation
276 buffer [50 mM Tris, 150 mM NaCl, 1% Nonidet P-40 (vol./vol.),
277 2 mM EGTA, 1 mM PMSF, 1 mM sodium orthovanadate, 2 mM
278 N-ethylmaleimide, 10% glycerol (vol./vol.), pH 7.4 at 22 °C].
279 An equal amount of proteins from lysates (~100 μg) was
280 resolved by SDS-PAGE (7.5–14% T SDS polyacrylamide gels)
281 under reducing conditions. All samples within an experi-
282 mental group were processed simultaneously to eliminate
283 inter-experimental variations. Proteins were transferred onto
284 nitrocellulose membranes and probed with primary anti-
285 bodies listed in Table 2. The blots were developed with an
286 enhanced chemiluminescence system using kits from Amer-
287 sham Pharmacia Biotech (Piscataway, NJ). Each immunoblot
288 experiment was repeated at least three times using different
289 sets of samples to obtain sufficient data for statistical
290 analysis. In selected experiments, immunoblots were probed
291 with a different antibody, namely the mouse anti-CAR
292 antibody instead of the rabbit antibody (see Table 2), which
293 yielded virtually identical results.

Fig. 3 – Changes in CAR expression in rat testes during testicular maturation. (A) Immunofluorescent staining of CAR (H-300) was performed on frozen sections of rat testes of different ages: 15- (a–d), 25- (e–h), and 60-day-old rats (i–l) vs. adult rat kidney (body weight, 300 g) (m–p). A mouse antibody against ZO-1 conjugated with FITC (green fluorescence) was used to localize the blood–testis barrier. Sections were then incubated with a donkey anti-rabbit Cy3-conjugated antibody to visualize CAR (red fluorescence). (m–p): Cross-section of frozen rat kidney was included to demonstrate the specificity of CAR staining. Signals of CAR staining co-localized with ZO-1 to tight junctions in the collecting tubules of rat kidney. At 15 days, when blood–testis barrier was absent and only spermatogonia were found in the seminiferous tubules, CAR staining was detected at the Sertoli–Sertoli and Sertoli–germ cell interface, surrounding cell nuclei. At day 25, CAR staining was observed to be co-localizing with ZO-1 to the newly formed blood–testis barrier, along with staining surrounding the acrosome region of late round spermatids. At day 60, when the rat testis matured with complete cycles of spermatogenesis, CAR staining were found at germ cells of all stages, yet the signals were most intense in early stage VIII tubules, where elongated spermatids anchor their heads to Sertoli cells in the epithelium. Signals were also detected at the blood–testis barrier, but not of the same intensity compared to those at the apical ectoplasmic specialization. Scale bar = 25 μm in (a), which also applies to (b–d) and (m–p). Scale bar = 50 μm in (e), which also applies to (f–l). (B) Immunohistochemical localization of CAR in the seminiferous epithelium was performed on frozen sections of testes from rats of different ages: 15- (a–c), 20- (d–f), 25-day-old rats (g–i); a, d, g are negative controls using normal rabbit IgG for each sample group. Scale bar = 50 μm in (b), which also applies to (e, h) and upper-right corner of (a, d, g). Scale bar = 25 μm in (a), which also applies to (c, d, f, g, i). (C) Immunoblot of CAR using testis lysates from rats of different ages. Brain lysate of 20-day-old rats served as a positive control. Bar graph summarizes results of three sets of immunoblots using separate batches of testis lysate preparation. The level of CAR in testes from 90-day-old rats was arbitrarily set at 1. (For interpretation of the references to colour in this figure legend, the reader is referred to the web version of this article.)

294 **Immunoprecipitation (IP)**

295 About 400 μg of proteins from testis or Sertoli cell lysates were
 296 used for IP. Sertoli cells were cultured alone for 4 days at
 297 0.5×10^6 cells/ cm^2 on Matrigel-coated dishes with established
 298 functional tight and anchoring junctions that mimicked the *in*
 299 *vivo* cellular physiology and morphology as earlier reported [23]
 300 prior to their used for lysate preparation. Testis or Sertoli cell
 301 lysates were first pretreated with 2 μg of rabbit or mouse IgG for
 302 approximately 1 h, followed by incubation with 10 μL Protein A/
 303 G-PLUS agarose (Santa Cruz, CA) for 2 h to eliminate non-
 304 specific binding of protein with IgG or agarose. After spinning
 305 down the agarose beads, supernatants were collected into new
 306 tubes for IP. 2 μg of primary antibody was added to this
 307 supernatant and incubated overnight. In negative controls,
 308 mouse or rabbit IgG of equivalent amount were applied in

substitute of primary antibodies. The immunocomplexes were 309
 then precipitated by incubating with 20 μL of Protein A/G Plus- 310
 Agarose for approximately 6 h. After that, the immunocom- 311
 plexes were washed four times with 300 μL washing buffer 312
 [50 mM Tris-HCl, 150 mM NaCl, 1% Nonidet P-40 (vol./vol.), 313
 1 mM EGTA, 1 mM PMSF, pH 7.4 at 22 $^\circ\text{C}$] by gentle 314
 re-suspension and mild centrifugation (5 min, 1000 $\times g$). Precipi- 315
 tated immunocomplexes were released from agarose beads by 316
 heating at 100 $^\circ\text{C}$ for 10 min in SDS-sample buffer [0.125 M Tris, 317
 pH 6.8 at 22 $^\circ\text{C}$, containing 1% SDS (wt./vol.), 1.6% 2- 318
 mercaptoethanol (vol./vol.), and 20% glycerol (vol./vol.)] for 319
 10 min. Proteins were then resolved by SDS-PAGE, and 320
 immunoblotting was performed as described in the previous 321
 section. Lysates from normal rat testes or Sertoli cells were 322
 used to serve as positive controls. We opted to use Sertoli cell 323
 lysates for co-IP instead of testis lysates for data reported 324



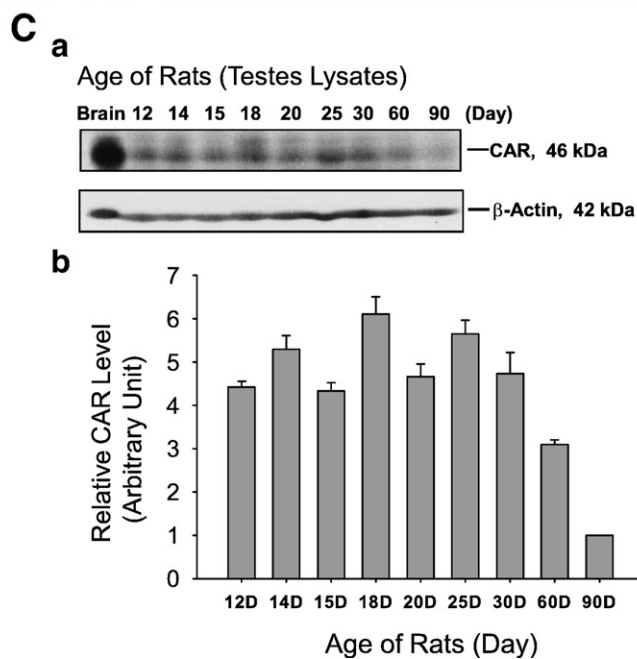
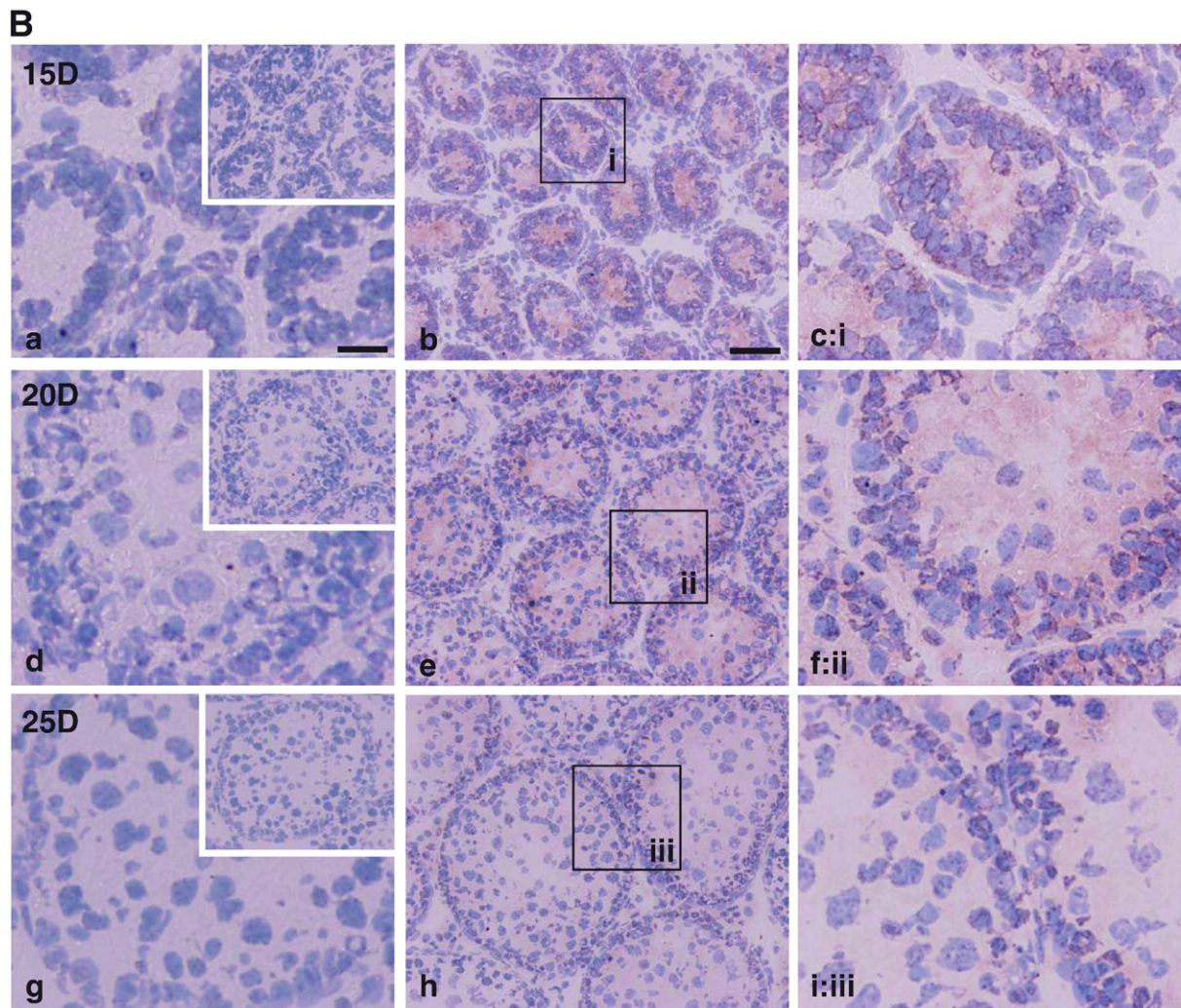


Fig. 3 (continued).

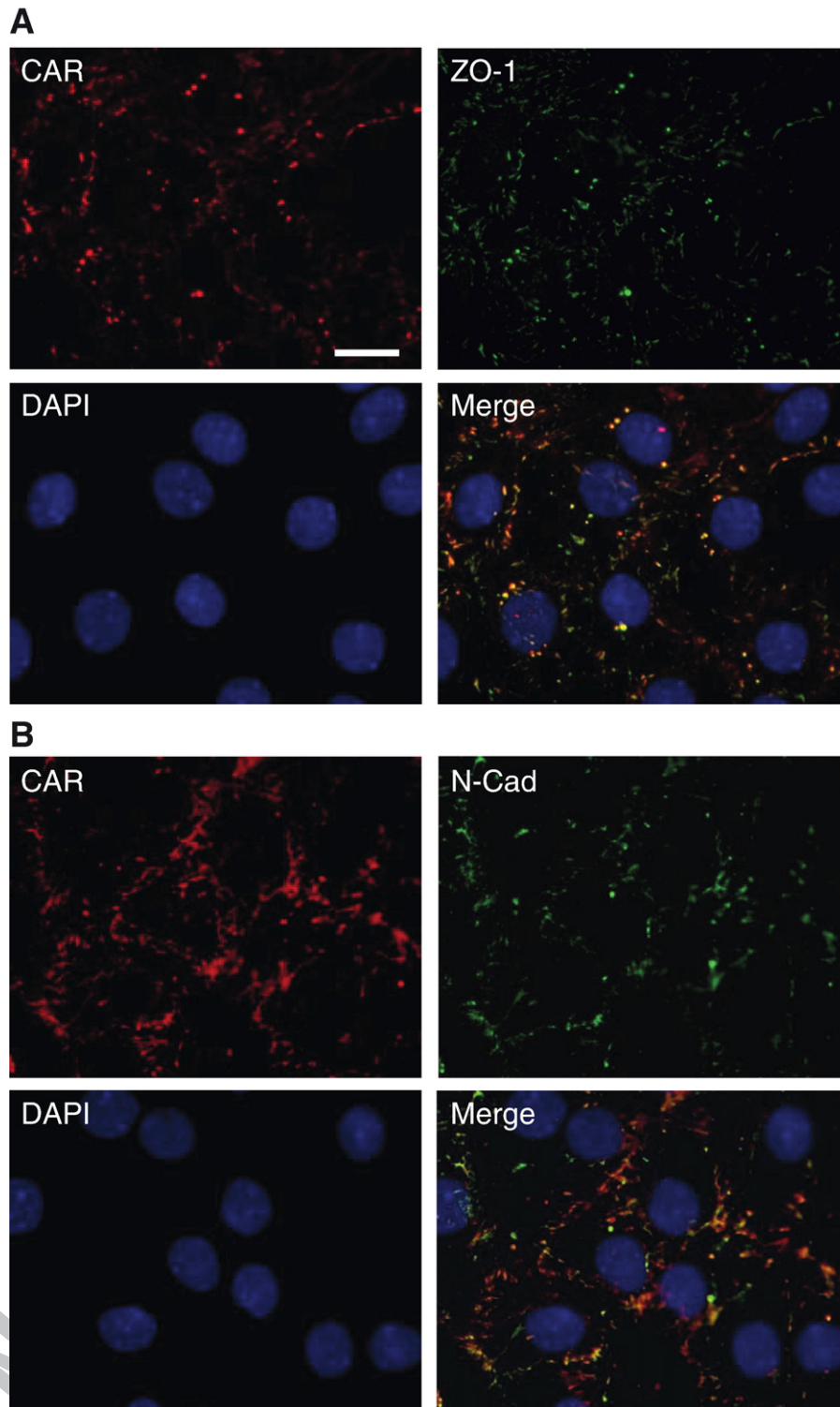


Fig. 4 – CAR localize at cell-cell contacts of Sertoli cells. Sertoli cells were cultured at low density (1×10^5 cells/cm²) for 3 days before staining. Areas of co-localization appear as orange. Immunofluorescent micrograph demonstrates that CAR was heavily concentrated at inter-Sertoli tight junctions, though staining occasionally was also seen close to the nucleus. (A) Cells were incubated with a rabbit anti-CAR polyclonal IgG as primary antibody, followed by a goat anti-rabbit CY3-conjugated secondary antibody. A mouse anti-ZO-1 FITC conjugate was used to locate inter-Sertoli tight junctions. (B) Cells were incubated with a rabbit anti-CAR (H-300) polyclonal antibody, along with a mouse anti-N-cadherin monoclonal antibody. N-Cadherin is a known component of the inter-Sertoli cell junctions at the blood-testis barrier. Scale bar=20 μ m in A, which also applies to B. This experiment was repeated at least 4 times over a period of 18 months using different batches of Sertoli cells where cultures were terminated on either day 2 ($n=2$) or day 3 ($n=2$), and similar results were obtained for all experiments. (For interpretation of the references to colour in this figure legend, the reader is referred to the web version of this article.)

325 herein to avoid results of protein–protein association between
326 CAR and other peripheral proteins that were derived from cells
327 in the interstitium (e.g., Leydig cells, macrophages, endothelial
328 cells in microvessels) and the tunica propria (e.g., peritubular
329 myoid cells, lymphatic cells).

330 Statistical analysis

331 Statistical analysis was performed using one-way ANOVA
332 using the GB-STAT Statistical Analysis Software package
333 (Version 7.0, Dynamic Microsystems, Inc., Silver Spring, MD).

334 Results

336 CAR is a product of both Sertoli and germ cells in rat testes

337 In order to examine the presence of CAR in normal rat testes,
338 we performed RT-PCR with total RNA extracted from Sertoli
339 cells and germ cells. These cell preparations were contami-
340 nated with a negligible number of other cells as described in
341 Materials and methods. S16 was co-amplified in all experi-
342 ments to confirm the correct composition of each reaction
343 mixture and the quality of mRNA. As the two isoforms of CAR
344 vary only at the cytoplasmic C-terminus, we designed a pair of
345 primers that flanked a large region in the extracellular
346 domain. As shown in Fig. 1A, sharp bands of expected size
347 (531 bp) were detected in both Sertoli and germ cells. This PCR
348 product was confirmed by direct nucleotide sequencing at
349 Genewiz (North Brunswick, NJ). Each of the three lanes of
350 Sertoli and germ cells in Fig. 1A represents RNA sample
351 prepared from separate batches of cells.

352 To test whether CAR is translated into a functional protein
353 in the testis, we carried out immunoblot analysis. As CAR is
354 most abundantly expressed in rat brains at the early develop-
355 ment stage [7], brain lysate from 20-day-old rats was included
356 as a positive control. When the immunoblot of Sertoli cell
357 lysate was probed with a rabbit anti-CAR (H-300) polyclonal
358 antibody, only one single prominent band was detected at
359 46 kDa (Fig. 1B), illustrating the specificity of the antibody. We
360 also examined the expression level of CAR in different cellular
361 fractions of the testis as shown in Fig. 1C. In comparison to
362 germ cells, Sertoli cells expressed a much higher level of CAR,
363 which contributed substantially to the amount of CAR protein
364 detected in lysates of rat seminiferous tubules. Fig. 1D is a
365 histogram representing densitometrically scanned results of
366 Fig. 1C, showing that the abundance of CAR in Sertoli cells is
367 approximately 6 times that of germ cells.

368 Localization of CAR in the seminiferous epithelium of adult rat 369 testes

370 Immunohistochemistry was used to examine the distribution
371 pattern of CAR in adult rat testes (Fig. 2A). Fig. 2B is a magnified
372 view of boxed area (a) in Fig. 2A, whereas Figs. 2C and D
373 correspond to boxed area (i) and (ii), respectively. CAR was seen
374 to be concentrated at the sites of apical ectoplasmic specializa-
375 tion of stage VIII seminiferous tubules, where elongated
376 spermatids anchor onto Sertoli cells before spermatogenesis.
377 Immunoreactive signals were discernible on round spermatids

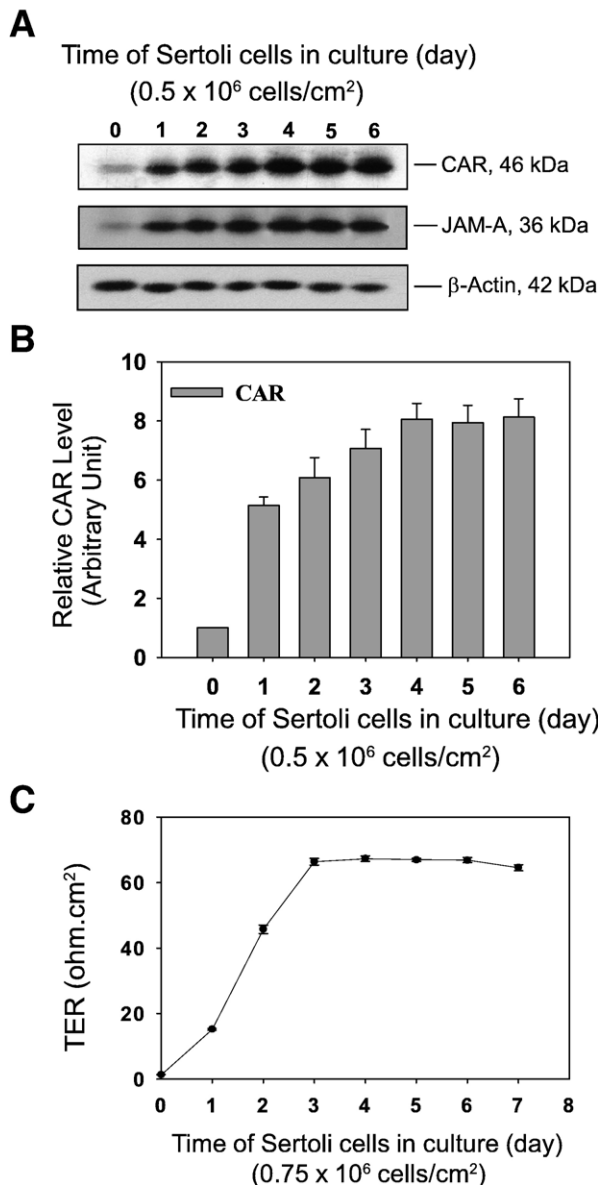
and early elongating spermatids as well, but the most intense
reddish-brown precipitates were localized to the convex side of
elongate spermatid heads (Figs. 2C and D). This observation is
in agreement with a recent report [18], in which signals from
immunofluorescent staining of CAR in rat seminiferous
tubules were found to be very pronounced in elongate
spermatids of stage VIII tubules. More importantly, our data
demonstrate that CAR expression was not restricted to germ
cells only. Robust signals were also detected along the basal
compartment of the seminiferous tubule, especially at the site
of the blood–testis barrier. In Figs. 2C and D, reddish-brown
precipitates of CAR were found near the basal lamina of the
seminiferous epithelium sitting side by side with sickle shaped
CAR staining at elongate spermatids. We also noticed minor
staining on Leydig cells, which is consistent with findings of
another research group [27]. Immunofluorescent studies (Fig.
2E) yielded similar results, showing the same staining pattern
as seen in Figs. 2A–D. Here, CAR signal appears as red, while
cell nuclei were stained blue with DAPI. Again, we observed
CAR residing at the convex side of elongate spermatid heads.
Fig. 2F serves as a negative control where cross-sections of
testes were incubated with purified rabbit IgG at the same
concentration as that of the primary antibody. No immunor-
eactivity was noticeable in the negative control, which verifies
the specificity of CAR (H-300) antibody. The results reported in
Figs. 2A–D by immunohistochemistry were also confirmed
using a different anti-CAR antibody raised in a goat (see Sup-
plementary Fig. 1), illustrating the localization of CAR in the
seminiferous epithelium as shown in Fig. 2 is specific to CAR.

CAR expression in rat testes changes during development

The expression of CAR is highly regulated during develop-
ment. In neonatal rats and mice, CAR was found to be
abundant in various tissues (e.g., heart, brain, skeletal
muscle), but its protein level would drop rapidly in adult
animals [7,28,29]. We thus sought to study the expression
pattern of CAR during testicular maturation. Immunofluor-
escent staining was performed on frozen sections of rat testes
of different ages. In 15-day-old rats (Figs. 3A, a–d), the blood-
testis barrier has not yet formed, CAR was seen to be
surrounding the nuclei of Sertoli cells and spermatogonia at
cell–cell interface. Signals of CAR (red) coincided with those of
ZO-1 (green) in most areas examined (Figs. 3A, c), suggesting
that CAR is implicated in the formation of the blood–testis
barrier. In 25-day-old postnatal rats, the blood–testis barrier
has already been established, as manifested by localization of
ZO-1 near the basal lamina of the seminiferous epithelium
(Figs. 3A, e–h). Here, CAR was observed to be associated with
spermatogonia, spermatocytes and round spermatids. Of note
is that elongating or elongate spermatids were absent in 25-
day-old rat testes. At the same time, modest CAR staining was
also found near the basal lamina of seminiferous tubules,
where it co-localized with ZO-1 at the blood–testis barrier
(Figs. 3A, e–h). By day 60 postnatal, rats are sexually mature,
with full epithelial cycles in the seminiferous tubules and
continuous waves of spermatogenesis. In cross sections of
adult rat testes, CAR staining appeared to be strongest in stage
VIII tubules, at the site of apical ES where elongate spermatids
anchor onto to Sertoli cells before spermatogenesis (Figs. 3A, i–

436 l). CAR signals also associated with spermatogonia and round
 437 spermatids near the basal compartment of the tubules.
 438 Distinct fluorescent signals of CAR were also detected at the
 439 blood-testis barrier (see Figs. 3A, i, k), which is identified by
 440 staining with mouse anti-ZO-1 FITC conjugate (see Figs. 3A, j).
 441 CAR and ZO-1 fluorescent signals were also co-localized in the
 442 seminiferous epithelium near the basement of the seminiferous
 443 tubules, consistent with their localization at the blood-
 444 testis barrier (Figs. 3A, k, l). In Figs. 3A, m-p, CAR clearly co-
 445 localized with ZO-1, which is expressed ubiquitously in the
 446 tight junctions of collecting tubules in a kidney nephron. This
 447 shall illustrate the specificity of CAR staining in the semi-
 448 niferous epithelium of the testis.

449 Micrographs in Fig. 3B are results of immunohistochem-
 450 istry studies using testes from rats at 15 day (a-c), 20 day (d-f),
 451 and 25 day (g-i) of age. These data support the distribution
 452 pattern of CAR seen in immunofluorescent staining. Figs. 3B
 453 (a, d, g) are negative controls for each sample group, in which
 454 normal rabbit IgG was used in substitute of polyclonal rabbit
 455 anti-CAR (H-300) antibody.



In addition, protein lysates of rat testes of different ages
 were analyzed by immunoblot (Fig. 3C). As shown in the bar
 chart (Figs. 3C, b), expression of CAR in rat testes was relatively
 high in neonatal rats and possibly being used to construct the
 blood-testis barrier at approximately 16 to 18 days of age.
 Overall, the CAR steady-state protein level in rat testes
 declined remarkably in adulthood. However, in comparison
 to other organs such as the brain, heart or muscle, where CAR
 level dropped by more than 100-fold after maturation, the drop
 in CAR protein level we observed in the testes is not as drastic.

CAR is localized at inter-Sertoli cell junctions *in vitro*

Sertoli cells isolated from 20-day-old rats were plated at low
 cell density at 0.1×10^6 cells/cm² to obtain confluent cell
 monolayers. Cells plated at high density often grow into an
 epithelium with overlapping cell layers, which would later
 affect the imaging of the cell-cell interface by fluorescent
 microscopy. Immunofluorescent staining was thus carried out
 after culturing Sertoli cells for 2 to 3 days (see Fig. 4 where cells
 were used for staining on day 3 following plating). By then,
 functional inter-Sertoli tight junction and adherens junctions
 were mostly established as shown by trans-epithelial electri-
 cal resistance measurement (TER) (Fig. 5) and electron
 microscopy [23]. CAR (red fluorescence) is observed to be
 concentrated at cell-cell contacts of Sertoli cells (Figs. 4A-B),
 exhibiting nearly identical localization pattern with tight
 junction marker ZO-1 (green fluorescence) and adherens
 junction protein N-cadherin (green fluorescence).

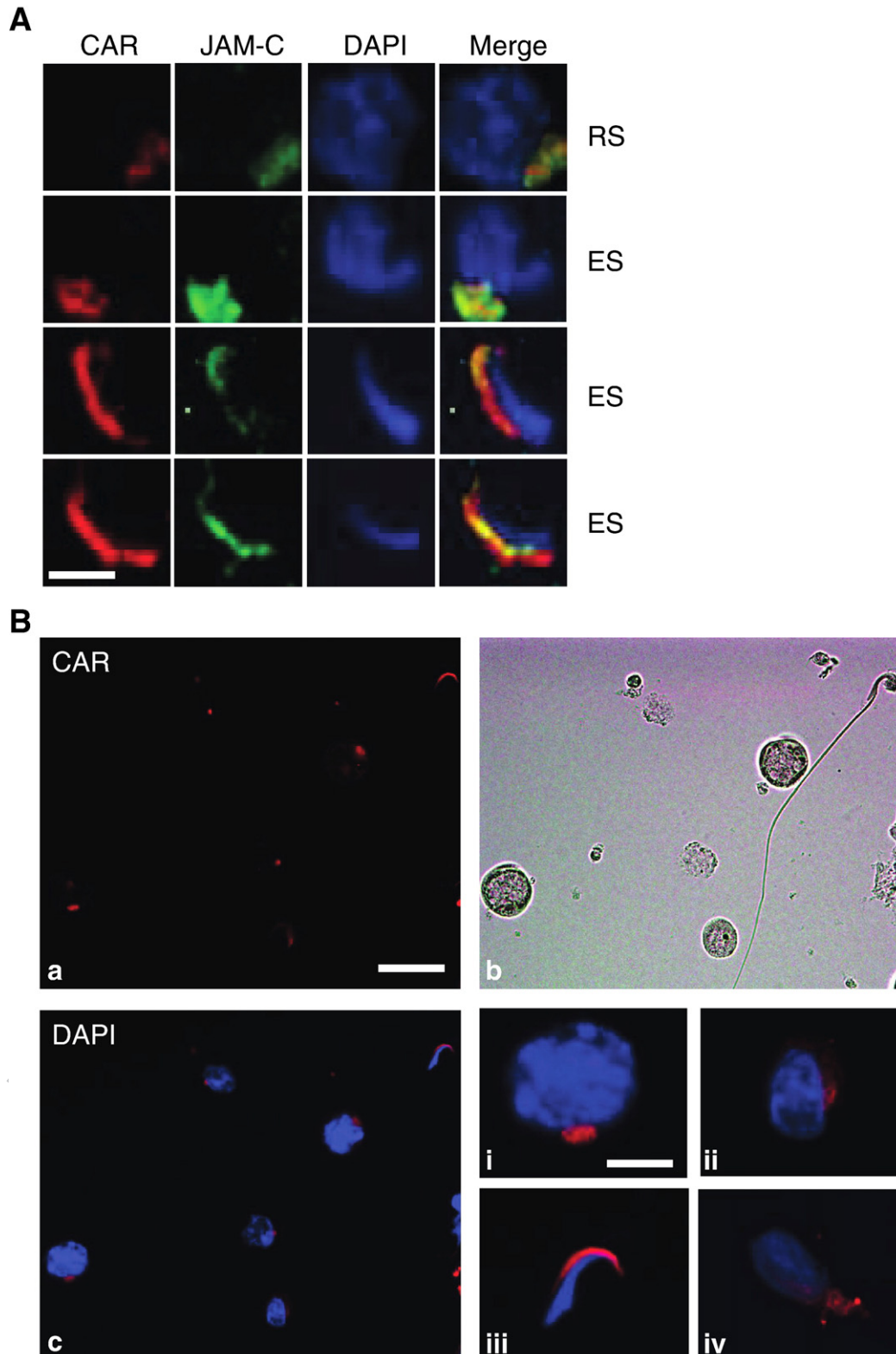
Induction of CAR in primary Sertoli cell cultures

Sertoli cells were isolated from 20-day-old rats and were
 plated at 0.5×10^6 cells/cm² on Matrigel-coated dishes. At this
 cell density, Sertoli cells were known to form a polarized

Fig. 5 – Induction of CAR during the assembly of inter Sertoli cell junctions *in vitro*. Sertoli cells were cultured at high density (0.5×10^6 cells/cm²) for 6 days. During this time course, an intact cell epithelium with functional tight junctions and adherens junctions were established and maintained. Cell cultures were terminated at specified time points. A steady increase in CAR expression level was detected by immunoblot. JAM-A served as a protein marker of tight junction, which also has an up-regulated expression level. (A) Immunoblots illustrating changes in the protein level of CAR and JAM-A. The same blot was also probed with β -actin to confirm equal protein loading. (B) Bar graph summarizes results from 3 sets of immunoblots using different batches of Sertoli cells. The steady-state protein level of CAR in Sertoli cells at time 0 was arbitrarily set at 1, against which one-way ANOVA was performed. * $P < 0.01$. (C) Transepithelial electrical resistance (TER) was measured at specific time points which assessed the establishment of the Sertoli cell tight junction-permeability barrier. Each time point had triplicate cultures, and each experiment was repeated 3 times using different batches of primary Sertoli cell cultures. TER reached its peak after about 4 days in culture and was maintained at that level thereafter.

487 epithelium that mimics the morphology and cellular behavior
 488 found *in vivo*, such as the physiological barrier maintained by
 489 tight junctions. Cultures were terminated at specific time
 490 points and lysed for protein extraction. As shown in Figs. 5A, B,
 491 at time 0, only a slight expression of CAR was detected by
 492 immunoblots right after Sertoli cell isolation, because rigorous

493 treatments with trypsin, collagenase and hyaluronidase in the
 494 isolation process could lyse most cell adhesion proteins that
 495 were used to maintain tissue organization. Expression level of
 496 CAR increased rapidly (i.e., about a 5-fold boost within 24 h)
 497 when Sertoli cells began to create clusters, gradually form and
 498 maintain an epithelium. CAR level peaked on day 4 and



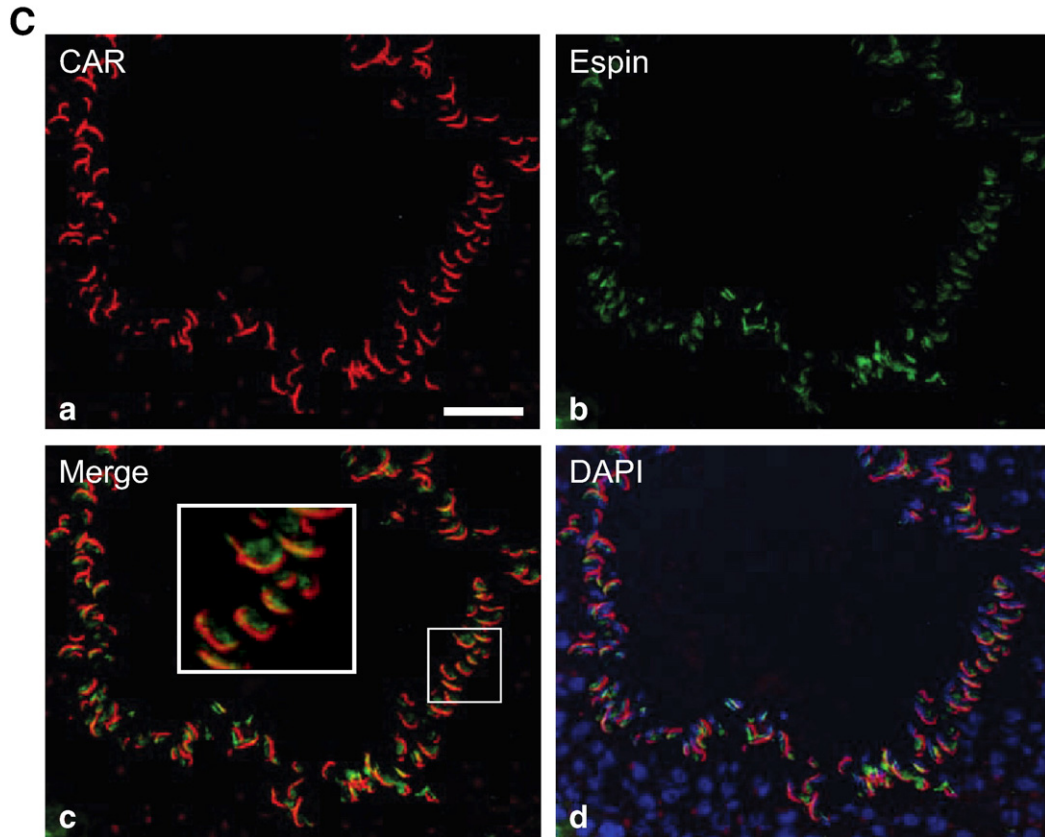


Fig. 6 – CAR is expressed by germ cells at different stages of differentiation. (A) Immunofluorescent staining of rat testes sections shows co-localization of CAR and JAM-C *in vivo*. Both proteins were found to be distributed on round spermatids and were confined to the heads of elongating/elongate spermatids. Scale bar = 5 μ m. (B) Rat germ cells were isolated by mechanical procedure (without glass wool), plated on poly-L-lysine-coated coverslips and permeabilized before staining. (a) Localization of CAR on germ cells: Immunofluorescent staining was performed on the slides with rabbit anti-CAR (H-300) polyclonal antibody, followed by incubation with Cy3-conjugated donkey anti-rabbit IgG. Scale bar = 25 μ m, which also applies to b and c. (b) Germ cells are visualized under light microscope. (c) Merged image of CAR and DAPI staining of nuclei. (i–iv) Magnified views of individual germ cells at different development stages: (i) spermatocyte, (ii) round spermatid, (iii) elongate spermatid (steps 17–18), (iv) elongating spermatid (steps 9–10). Scale bar = 5 μ m in (i), which also applies to (ii–iv). (C) Immunofluorescent micrographs of a stage VIII seminiferous tubule. CAR (red) was stained with a rabbit anti-CAR (H-300) polyclonal antibody and espin (green) was stained with a mouse anti-espin monoclonal antibody. Merged image (c) shows that CAR and espin were co-localized to the apical ES site in the seminiferous epithelium. Scale bar = 50 μ m. (For interpretation of the references to colour in this figure legend, the reader is referred to the web version of this article.)

499 remained plateau thereafter. JAM-A, another tight junction-
 500 associated protein, was also seen to be significantly induced
 501 during the assembly of inter-Sertoli cell junctions (Figs. 5A–B).
 502 The increase of CAR expression correlated with a rise in TER
 503 readings, which were used to assess the establishment of the
 504 inter-Sertoli cell tight junction permeability barrier (Fig. 5C).
 505 These data suggest that CAR is indeed a building block of inter-
 506 Sertoli cell junctions at the blood–testis barrier including tight
 507 junctions and basal ectoplasmic specialization.

508 CAR is expressed by germ cells at different stages of 509 differentiation

510 In a recent paper, CAR was found to be localized to the
 511 acrosome region of mature spermatozoa isolated from mouse

epididymis and human ejaculate [18]. From our immunohis- 512
 tochemistry and immunofluorescent microscopy studies on 513
 rat testes sections, we noticed that CAR staining was asso- 514
 ciated with spermatogonia, spermatocytes, round spermatids 515
 as well as elongate spermatids. Immunofluorescent staining of 516
 adult rat testes sections has also co-localized CAR with JAM-C 517
in vivo (Fig. 6A). Both proteins were found to be distributed on 518
 round spermatids and were confined to elongating/elongate 519
 spermatid heads later on. To gain a more accurate picture of 520
 CAR expression during germ cell differentiation, we conducted 521
 immunofluorescent staining with germ cells alone. The 522
 isolation process of germ cells was purely mechanical and 523
 glass wool filtration step was omitted. Therefore the final 524
 product contained germ cells at all stages of differentiation, 525
 including spermatogonia, spermatocytes, round spermatids, 526

527 elongating and elongate spermatids at a relative ratio similar
 528 to that of germs cells found in the seminiferous epithelium *in*
 529 *vivo* [24]. Germ cells were plated onto poly-L-lysine-coated
 530 coverslips and permeabilized with 0.1% Triton X-100. Data
 531 shown in Fig. 6B illustrated the presence of CAR in spermatocytes
 532 (i), round spermatids (ii), elongating spermatids (iv) and
 533 elongate spermatids (iii). In round spermatids, CAR staining
 534 appears to be at the site of early acrosome. In elongate and
 535 elongating spermatids, immunoreactive signals are concentrated
 536 at the convex surface of spermatid heads, which is the site of
 537 late acrosome as well as the apical ectoplasmic specialization
 538 (Figs. 6B, a, b, c and i-iv). A micrograph from transillumination
 539 microscopy was presented in Figs. 6B, b to show the morphology
 540 of germ cells.

541 CAR co-localized with espin at the apical ectoplasmic 542 specialization (apical ES)

543 CAR has previously been localized to the acrosome in mature
 544 spermatozoa of mice and human [18]. Since acrosome/
 545 acrosomal membrane and plasma membrane at the apical
 546 ES are intimately associated structures, it is not known if the
 547 findings reported above (e.g., Figs. 2 and 3) represent the
 548 localization of CAR at the apical ES. In order to define the
 549 precise ultrastructural location of CAR on germ cells, immunogold
 550 electron microscopy studies were performed at the Rockefeller
 551 University Bio-imaging Resource Center. However, we encountered
 552 technical difficulties with both antibodies (Table 2). We then
 553 turned to fluorescent microscopy using double staining technique
 554 to assess the co-localization of CAR with espin at the apical
 555 ES in the seminiferous epithelium in adult rat testes (Fig. 6C).
 556 Espin is a known protein marker of ectoplasmic specialization
 557 (for a review, see [33]) contributed by Sertoli cells (Fig. 6C).
 558 Red fluorescence signals of CAR (Figs. 6C, a) appeared to
 559 co-localize with the green fluorescence signals from espin
 560 (Figs. 6C, b) near the luminal edge of the seminiferous
 561 epithelium in a stage VIII tubule, where elongate spermatids
 562 anchored onto Sertoli cells before spermatogenesis (Figs. 6C,
 563 c, d). Due to the limited resolution of immunofluorescent
 564 imaging, data from this study are still not sufficient to
 565 distinguish between the two locations (i.e. the plasma
 566 membrane and the acrosome/acrosomal membrane). It is
 567 possible that CAR is expressed on both sites, namely the
 568 acrosome membrane and the apical ES structure. From
 569 immunohistochemistry and immunofluorescence studies on
 570 testes from 15-day-old rats, we observed that CAR staining
 571 surrounding the nuclei of spermatogonia and Sertoli cells
 572 (Figs. 3A-B). In 15-day-old rats, only spermatogonia were
 573 present in the seminiferous epithelium of pups. Considering
 574 that spermatogonia are non-polarized stem cells without
 575 acrosome structures, significant CAR staining surrounding the
 576 nuclei of spermatogonia favors the notion that CAR is
 577 present on the plasma membrane of germ cells.

579 TNF α treatment down-regulated CAR protein level in Sertoli 580 cell culture

581 Sertoli cells were cultured for 4 days alone to allow the
 582 formation of an epithelium with functional tight junction

583 permeability barriers. Also the endogenous target gene
 584 expression pertinent to tight junction barrier assembly would
 585 be subsided by then. On day 5, F12/DMEM medium containing
 586 20 ng/mL recombinant human TNF α were added onto these
 587 cultures and cells were terminated at specified time points
 588 (see Fig. 7). Medium containing the same amount of TNF α
 589 was changed every 24 h afterwards. By immunoblot analysis,
 590 we observed a significant drop in CAR level by days 2 and 3
 591 after TNF α treatment (Figs. 7A-B). However, this response
 592 to cytokine treatment was not very significant in comparison
 593 to that of occludin and JAM-A, which displayed a dramatic
 594 decrease after only 4 h of treatment.

595 Association of CAR with other proteins examined by co-IP

596 For co-IP experiments, Sertoli cells were cultured alone for
 597 ~4 days and terminated for lysate preparation. A rabbit

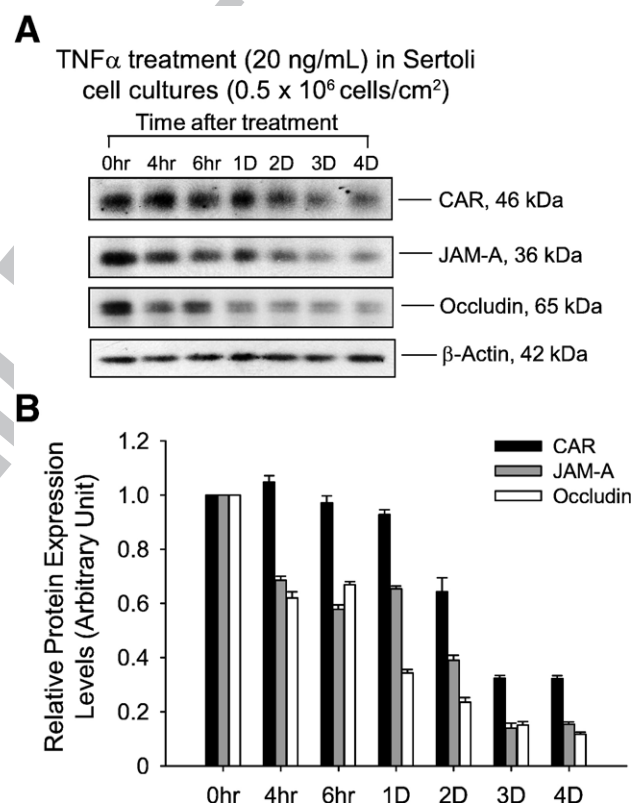


Fig. 7 – TNF α treatment down-regulated CAR protein level in Sertoli cell culture. Sertoli cells were cultured for 4 days prior to their use for this experiment as described in Materials and methods. Culture medium (F12/DMEM) was supplemented with TNF α (20 ng/mL) on day 5 and thereafter. Cultures were terminated at specified time points and processed for immunoblot analysis. (A) CAR protein level decreased by 2 to 3 days after TNF α treatment, whereas the level of occludin and JAM-A dropped significantly by 4 h after TNF α treatment. (B) Bar chart summarizes results from 3 sets of immunoblot using different batches of Sertoli cell cultures. The steady-state protein level of the target protein at time 0 was arbitrarily set at 1, against which one-way ANOVA was performed. ns, not significantly different; * $P < 0.05$; ** $P < 0.01$.

598 monoclonal antibody against Src-kinase family was used as a
599 precipitating antibody to incubate with Sertoli cell lysate.
600 Immunocomplexes were separated by SDS-PAGE, transferred
601 to nitrocellulose membrane and probed with a mouse anti-
602 CAR antibody. Normal rabbit IgG was used in negative
603 controls. We clearly detected a band at 46 kDa in lysates of
604 Sertoli cells that were incubated with a rabbit monoclonal
605 antibody against Src kinase family. A much stronger band of
606 the same size was identified in positive control where rabbit
607 anti-CAR (H-300) was used for precipitation (Fig. 8A). This
608 suggests that CAR was associated with members of Src kinase
609 family via direct or indirect interactions. The anti-Src antibody
610 (see Table 2) was shown to react specifically to Src as
611 illustrated in an immunoblot experiment (Fig. 8B). To further
612 verify that CAR is indeed structurally interacting with proteins
613 of Src kinase family, we next conducted immunofluorescent
614 microscopy studies on Sertoli cells in culture for 3 days at low
615 density (0.1×10^6 cells/cm²) to assess co-localization of CAR
616 and Src. As shown in Fig. 8C, CAR (red fluorescence) was
617 indeed co-localized with c-Src (green fluorescence), both of
618 which reside at the cell–cell interface (d vs. a–c in Fig. 8c). It is
619 possible that CAR might also co-localize with other members
620 of the Src kinase family, such as v-Src or Fyn, which we have
621 not examined in this study.

622 In order to expand the observation reported in Fig. 8A
623 regarding other binding partners for CAR, we also included
624 antibodies against other protein adaptors and kinases known
625 to affect tight and anchoring junction dynamics in Sertoli cells
626 (Figs. 8D–E). In this co-IP experiment, vinculin, and β -catenin
627 were also identified to be the putative interacting partners of
628 CAR besides Src. Fig. 8E summarizes results of this co-IP study,
629 including both positive and negative data.

630 Discussion

632 CAR is strongly expressed in multiple tissues during the
633 embryonic and neonatal phase of rats and mice, but its level
634 attenuated substantially in brains, hearts and became unde-
635 tectable in muscles of adult animals [3,4,7]. The high
636 abundance of CAR during embryonic and neonatal periods
637 has been ascribed to its role in mediating cell adhesion during
638 tissue morphogenesis [4,6,7]. In adult rat testes, extensive
639 restructuring of cytoarchitecture occurs continuously at
640 different stages of seminiferous epithelial cycle [13], which
641 enables the translocation of developing germ cells from the
642 basal to the adluminal compartment. In this respect, mature
643 testis does undergo developmental changes which resemble
644 those occurring in other organs during tissue genesis [30]. The
645 persistent expression of CAR in adult rat testes indicates that
646 it might serve an important role in spermatogenesis as a cell
647 adhesion molecule.

648 Our data from cell culture experiments show that CAR
649 resides at the inter-Sertoli cell contacts, co-localizing with
650 tight junction marker ZO-1 as well as adherens junction
651 protein N-cadherin. Furthermore, we detected an induction of
652 CAR during the formation of a functional Sertoli cell epithe-
653 lium *in vitro*. These findings are in agreement with previous
654 reports that CAR is an integral membrane component of tight
655 junction or adherens junction, and potentially a homophilic

656 adhesion molecule [7–9]. *In vivo* data from immunofluores-
657 cence and immunohistochemistry studies localized CAR to
658 the site of blood–testis barrier in rats. Based on these
659 observations, we propose that CAR is a building block of the
660 inter-Sertoli junctions at the blood–testis barrier.

661 We also identified CAR expression on isolated germ cells,
662 including spermatogonia, spermatocytes, round spermatids
663 and elongate spermatids. Detailed description of CAR loca-
664 lization in spermatozoa was given in a recent paper [18].
665 Taken together, we concluded that CAR is constitutively
666 expressed by germ cells during spermatogenesis, starting
667 from spermatocytes to spermatozoa. The presence of CAR at
668 opposing surfaces of both Sertoli and germ cells introduces
669 the possibility that homotypical CAR interaction might take
670 place. Structural analysis revealed that CAR form homodimer
671 in crystal and in solution via D1 domains, the distal one of its
672 two extracellular Ig-like loops [31]. Interestingly, fiber knob
673 projecting from adenovirus capsid binds to CAR through the
674 same interface, but at a higher affinity [31,32]. Viral fiber
675 knob competes with CAR to interrupt cell–cell adhesions, not
676 only for virus attachment [1,10], but also to spread viral
677 particles from infected cells. To reach the airway lumen for
678 further infection, adenovirus released at the basolateral side
679 of the human airway epithelia must escape through adjacent
680 cells to emerge on the apical cell surface. Viral fiber knobs
681 facilitate this escape by competitive inhibition of CAR–CAR
682 interactions, which either perturb junctional complex
683 mechanically or trigger a signaling cascade to disintegrate
684 the entire cell junction [9]. The breakthrough of viral
685 pathogens across tissue barriers is highly reminiscent of
686 germ cells traversing the seminiferous epithelium [13], which
687 requires breakdown of existent inter-Sertoli junctions and
688 instant assembly of inter Sertoli–germ adherens junctions
689 [33]. In this scenario, CAR expressed on differentiating germ
690 cells could interact with CAR on the Sertoli cell side,
691 replacing the original inter-Sertoli cell CAR: CAR homodimer.
692 During viral infection, it has been postulated that after
693 binding with CAR, the adenovirus fiber-knob triggers a
694 cytokine response to compromise the integrity of airway
695 junctions [34]. It is attractive to speculate that CAR on the
696 Sertoli cell side may have the same signaling properties to
697 open up inter-Sertoli cell junctions, thus allowing the
698 passage of germ cells.

699 Of particular interest is whether CAR presented on the
700 Sertoli cell surface would have heterotypical interaction with
701 JAM-C expressed on the opposing germ cell surface, since JAM-
702 C and CAR have been co-immunoprecipitated from mouse
703 testes [18]. Transmembrane proteins of the immunoglobulin
704 family have been known to confer adhesion between Sertoli
705 and germ cells via heterotypical interactions. For example,
706 nectin-2 and nectin-3 form heterotypical complex at the
707 Sertoli–spermatid interface [35], and likewise JAM-B on the
708 Sertoli cell side interact with JAM-C on spermatids in mouse
709 testes [17]. In this study, we were not able to immunopreci-
710 pitate CAR with JAM-C using protein lysate from rat testes or
711 Sertoli cells. This might be due to the titer or binding
712 specificity of our antibodies. However, we did characterize
713 the co-localization of JAM-C and CAR in rat testes at the site of
714 apical ectoplasmic specialization, where Sertoli–spermatid
715 junctions are present.

716 In other cell types, for example, JAM-C has been observed to
 717 mediate neutrophil migration through the endothelium [11].
 718 Likewise, JAM-like protein on neutrophils and CAR on T84
 719 monolayer were found to promote the trans-epithelial migra-
 720 tion of neutrophils by adhesive interactions [25]. Similar
 721 mechanisms could be utilized by developing preleptotene
 722 spermatocytes to migrate through the tight junctions between
 723 adjacent Sertoli cells, with CAR on the Sertoli cell surface
 724 interacting with JAM-C on the germ cell surface. Needless to
 725 say, this notion has to be vigorously investigated in future
 726 studies.

727 During cytokine treatment (TNF α at 20 ng/ml) of Sertoli
 728 cells in culture, we observed a decline in CAR level.
 729 Inflammatory cytokines, such as TNF α , TGF β and IFN γ , are
 730 known to compromise epithelial integrity by repressing cell-
 731 cell adhesion molecules (e.g. E-cadherin, ZO-1 and CAR) [36-
 732 38]. Reduced expression of CAR or E-cadherin was most
 733 evident among carcinomas under progression, which was
 734 frequently accompanied by cytokine response *in vivo* [39,40].
 735 In the testes, TNF α is secreted by both Sertoli and germ cells
 736 [41,42]. Our group has conducted several studies on cytokine-
 737 mediated restructuring of the junctional complex in sperma-
 738 togenesis [41,43-45]. We found that TNF α is capable of
 739 perturbing Sertoli-cell tight junction barrier assembly *in vitro*
 740 dose dependently [41]. Recently we reported that TNF α is also
 741 a regulator of Sertoli-Sertoli and Sertoli-germ cell junctional
 742 dynamics *in vivo* [46]. Localized production of TNF α from
 743 Sertoli and germ cells into the microenvironment at the basal
 744 compartment of seminiferous tubule may induce an "open-
 745 ing" of inter-Sertoli cell junctions by down-regulating tight
 746 junction proteins occludin and ZO-1 [46]. With this knowl-
 747 edge, we might be able to understand the physiology of CAR
 748 decrease in Sertoli cell culture after TNF α treatment. It is
 749 notable that occludin and JAM-A responded to TNF α treat-
 750 ment far more rapidly than CAR in Sertoli cell culture. After

only 4 h of treatment, we saw a significant decline in the level
 of occludin and JAM-A, in comparison to the time interval of 2
 to 3 days before we detected a decline in CAR level. In some
 types of cells, such as human airway epithelia, CAR was
 located within the adherens junctions at the basolateral side
 of the columnar cell layer, rendering the cells resistant to viral
 infection from the apical surface [47]. Here, it is not certain
 whether CAR also resides near the basal side of the Sertoli cell
 layers as it does in human airway epithelia. If that were the
 case, we might be able to explain its slow response to
 cytokine treatment applied from the surface of the Sertoli cell
 culture.

Through immunoprecipitation experiments, we identified
 the protein complex of CAR and Src family kinase in Sertoli
 cell lysate. Immunofluorescent studies did co-localize CAR
 with c-Src in Sertoli cell culture. The rabbit monoclonal
 antibody used for immunoprecipitation was targeted
 towards Src kinase family, so we did not assign a specific
 Src kinase that associated with CAR. Notably, the cytoplas-
 mic tail of CAR does contain one putative tyrosine phos-
 phosphorylation site [48]. Src kinases were known to interact
 with other adhesion molecules at the Sertoli-germ cell interface,
 including β_1 -integrin [49] and laminin γ_3 [29]. It is concei-
 vable that Src kinase also interacts with CAR directly or
 indirectly to mediate signal transduction between Sertoli-
 Sertoli or Sertoli-germ cells. A recent article beautifully
 illustrated the mechanism of coxsackievirus invasion of
 tight junctions through CAR, demonstrating that Src kinase
 (Fyn) activation is an essential signaling event for viral
 internalization via caveolin-1 [50]. This poses an intriguing
 question of how Src kinase activity regulates germ cell
 movement along Sertoli cells. We also identified the inter-
 action of CAR with vinculin and β -catenin in Sertoli cell
 lysates, the latter of which has already been reported as a
 putative binding partner of CAR in other epithelia [9]. But the

Fig. 8 – Association between CAR and different adaptors and kinases in Sertoli cells cultured *in vitro*. Sertoli cells were cultured for 4 days at 0.5×10^6 cells/cm² that permitted the establishment of functional tight and anchoring junctions, which also mimicked the functional physiology and morphology of Sertoli cells *in vivo*, prior to their use for lysate preparation. (A) Co-IP experiments revealed the interaction between CAR and Src kinase in Sertoli cell lysates. 500 μ g of Sertoli cell lysates were prepared and immunoprecipitated with rabbit monoclonal antibody towards Src kinase family. The immunocomplexes were then subject to immunoblot analysis and incubated with a mouse anti-CAR monoclonal antibody. Rabbit anti-CAR polyclonal antibody and normal rabbit IgG were also used as precipitating antibodies for the Co-IP experiments, serving as a positive and negative control, respectively. "Rb" stands for rabbit. (B) A single prominent band corresponding to the apparent Mr of Src family protein kinase at 60 kDa was detected on the immunoblot using Sertoli cell lysate (100 μ g protein), demonstrating the specificity of the antibody. (C) Immunofluorescent staining reveals the co-localization of CAR with c-Src. Sertoli cells were cultured at low density (0.1×10^6 cells/cm²) for 3 days prior to use for fluorescent microscopy. Cells were incubated with a rabbit anti-CAR polyclonal IgG and a mouse anti-c-Src monoclonal IgG as primary antibody, followed by a donkey anti-rabbit CY3 (red fluorescence)-conjugated secondary antibody (a) and a donkey anti-mouse FITC (green fluorescence)-conjugated secondary antibody (b). Both proteins were seen to reside at cell-cell interface (a, b). Nuclei were visualized by DAPI staining (c). Areas of co-localization appear as orange (d). Scale bar=30 μ m in a, which applies to b-d. (D-E) Aside from Src, we also performed co-IP studies with antibodies against other adaptors and protein kinase. In the blot shown in D, the immunocomplexes were subject to immunoblot analysis and incubated with a mouse anti-CAR monoclonal antibody. Lysates from Sertoli cells were loaded onto the same gel to illustrate the specificity of the antibody and served as positive control (+ve Ctrl). (E) Tabulated co-IP results using different antibodies against protein adaptors and kinases present in Sertoli cells. Antibodies that failed to pull down CAR were also listed here. The immunocomplexes were separated by SDS-PAGE and probed with different CAR antibodies in immunoblots. The results shown here have been repeated three times using different batches of Sertoli cell cultures. "+", positive co-IP result; "-", negative co-IP result. (For interpretation of the references to colour in this figure legend, the reader is referred to the web version of this article.)

786 direct or indirect interaction between CAR and vinculin
787 require further investigation.

788 In summary, our study revealed the presence of CAR in rat
789 Sertoli cells and its localization at intercellular junctions. We
790 also identified CAR on isolated germ cells, including sperma-
791 togonia spermatocytes, round spermatids and elongate sper-
792 matids. The multifaceted nature of this protein was best
793 manifested by its localization at the blood-testis barrier of the
794 Sertoli-Sertoli cell interface as well as the apical ectoplasmic

795 specialization at the Sertoli-germ cell interface. This suggests
796 that CAR not only serves to maintain inter-Sertoli cell
797 junctional barrier but could also be acting in concert with
798 other protein complexes to facilitate germ cell movement at
799 the Sertoli-germ cell interface. It is possible that the same
800 receptor utilized by viral pathogens to breakthrough the
801 epithelial barrier was also employed by germ cells to migrate
802 through the seminiferous epithelium during spermatogenesis.
803 Our data from immunoprecipitation and TNF α treatment of

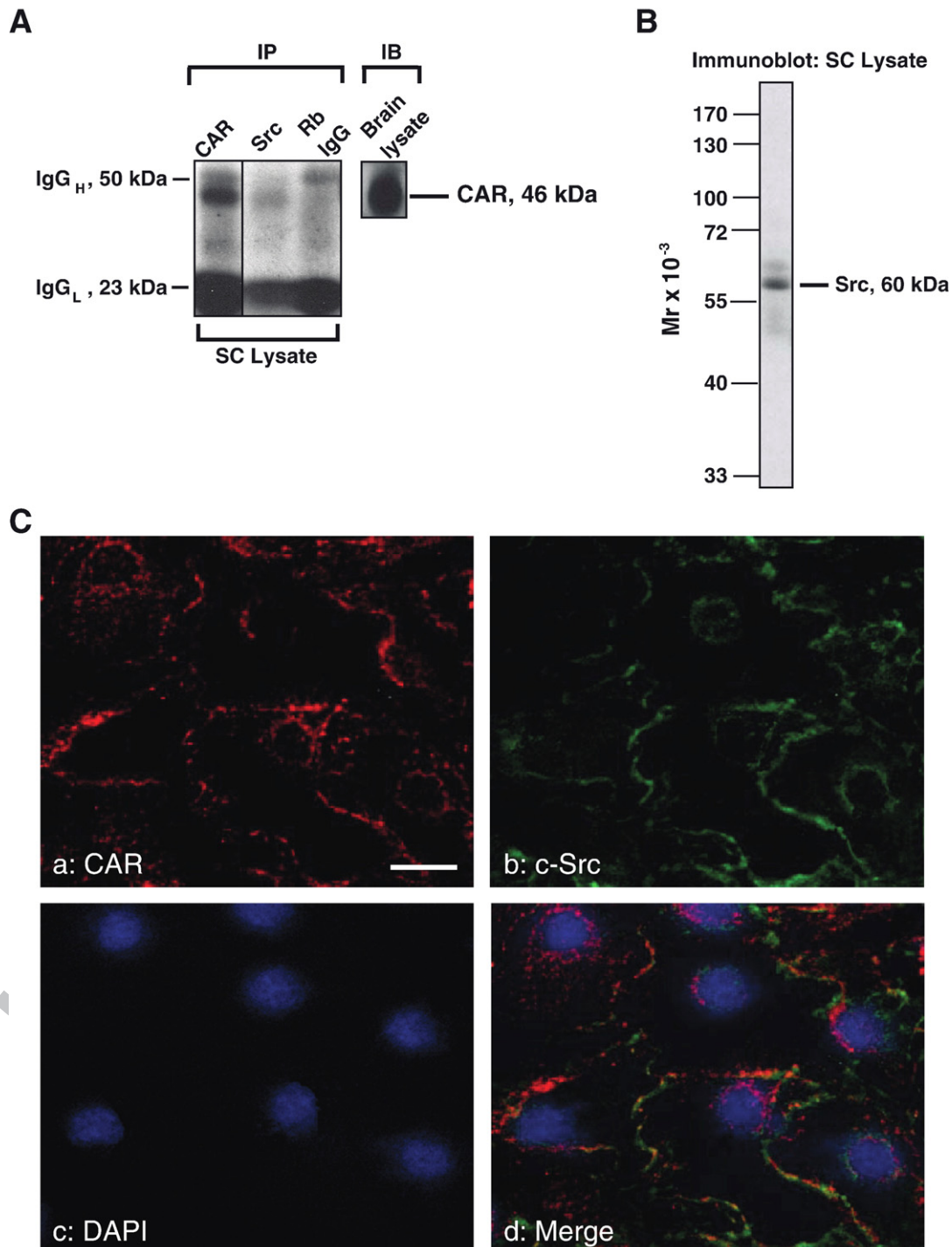
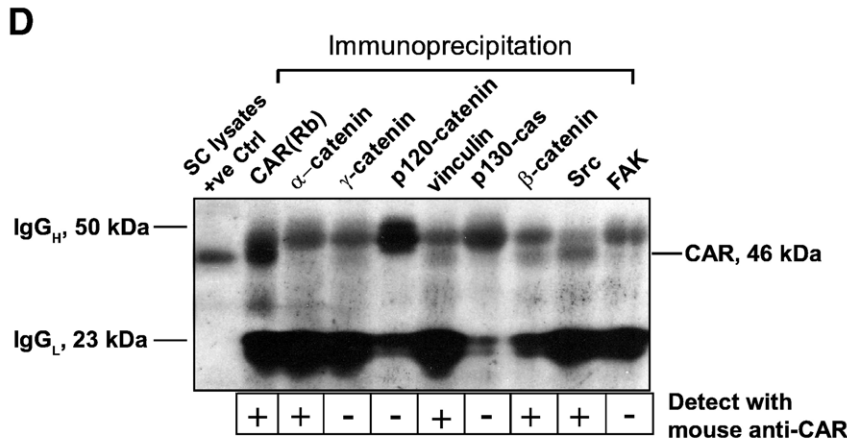


Fig. 8.



E Association of CAR with other proteins examined by Co-IP

	Precipitating Antibody	Animal Source	Cat. No.	Lot No.	Vendor	IB with CAR (Rabbit)	IB with CAR (Mouse)	IB with CAR (Goat)
Membrane proteins	CAR	Rabbit	sc-15405	J1304	Santa Cruz	+	+	+
	CAR	Mouse	sc-32795	E2605	Santa Cruz	+	+	-
	CAR	Goat	sc-10313	F0304	Santa Cruz	-	-	-
	β 1-integrin	Mouse	610486	53855	BD Transduction Laboratories	-	-	-
Adaptors	α -catenin	Rabbit	sc-7894	A2705	Santa Cruz	-	-	-
	β -catenin	Rabbit	sc-7199	F0204	Santa Cruz	+	+	+
	γ -catenin	Rabbit	sc-7900	J139	Santa Cruz	-	+	-
	p120-catenin	Mouse	sc-23873	D2104	Santa Cruz	-	-	-
	Vinculin	Rabbit	sc-5573	I2204	Santa Cruz	+	+	+
	α -actinin	Goat	sc-7453	D292	Santa Cruz	-	-	-
	p130 cas	Rabbit	06500	19950	Upstate	-	-	-
	p-paxillin	Goat	sc-14035	H311	Santa Cruz	-	-	-
Kinases	Src	Rabbit	05-772	26812	Upstate	+	+	+
	PI-3 kinase	Rabbit	06497	25006	Upstate	-	+	+
	FAK	Rabbit	sc-558	D1806	Santa Cruz	-	-	-

Fig. 8 (continued).

804 Sertoli cell cultures supports, but does not prove, the potential
 805 role for CAR in promoting germ cell migration. Work is in now
 806 progress to pursue this idea.

808 Acknowledgments

809 This work was supported in part by grants from the National
 810 Institutes of Health (NICHD U01 HD045908; U54 HD29990
 811 Project 3 to CYC), the CONRAD Program (CICCR, CIG 01-72 to
 812 CYC), and the Hong Kong Research Grant Council (HKU 7536/
 813 05M to WML).

Appendix A. Supplementary data

814

Supplementary data associated with this article can be found,
 816 in the online version, at [doi:10.1016/j.yexcr.2007.01.017](https://doi.org/10.1016/j.yexcr.2007.01.017).
 817

REFERENCES

818

[1] J.M. Bergelson, J.A. Cunningham, G. Droguett, E.A. Kurt-Jones, 819
 A. Krithivas, J.S. Hong, M.S. Horwitz, R.L. Crowell, R.W. 820
 Finberg, Isolation of a common receptor for coxsackie B 821
 822

- viruses and adenoviruses 2 and 5, *Science* 275 (1997) 1320–1323.
- [2] J.M. Bergelson, Receptors mediating adenovirus attachment and internalization, *Biochem. Pharmacol.* 57 (1999) 975–979.
- [3] M. Sinnreich, C.A. Shaw, G. Pari, J. Nalbantoglu, P.C. Holland, G. Karpati, Localization of coxsackie virus and adenovirus receptor (CAR) in normal and regenerating human muscle, *Neuromuscul. Dis.* 15 (2005) 541–548.
- [4] D.R. Asher, A.M. Cerny, S.R. Weiler, J.W. Horner, M.L. Keeler, M.A. Neptune, S.N. Jones, R.T. Bronson, R.A. DePinho, W., F.R., Coxsackievirus and adenovirus receptor is essential for cardiomyocyte development, *Genesis* 42 (2005) 77–85.
- [5] A. Nasuno, K. Toba, T. Ozawa, H. Hanawa, Y. Osman, Y. Hotta, K. Yoshida, T. Saigawa, K. Kato, R. Kuwano, Expression of coxsackievirus and adenovirus receptor in neointima of the rat carotid artery, *Cardiovasc. Pathol.* 13 (2004) 79–84.
- [6] E. Raschperger, J. Thyberg, S. Pettersson, L. Philipson, J. Fuxe, R.F. Pettersson, The coxsackie- and adenovirus receptor (CAR) is an *in vivo* marker for epithelial tight junctions, with a potential role in regulating permeability and tissue homeostasis, *Exp. Cell Res.* 312 (2006) 1566–1580.
- [7] T. Honda, H. Saitoh, M. Masuko, T. Katagiri-Abe, K. Tominaga, I. Kozakai, K. Kobayashi, T. Kumanishi, Y.G. Watanabe, S. Odani, R. Kuwano, The coxsackievirus–adenovirus receptor protein as a cell adhesion molecule in the developing mouse brain, *Mol. Brain Res.* 77 (2000) 19–28.
- [8] C.J. Cohen, J.T.C. Shieh, R.J. Pickles, T. Okegawa, J.-T. Hsieh, J.M. Bergelson, The coxsackievirus and adenovirus receptor is a transmembrane component of the tight junction, *Proc. Natl. Acad. Sci. U. S. A.* 98 (2001) 15191–15196.
- [9] R.W. Walters, P. Freimuth, T.O. Moninger, I. Ganske, J. Zabner, M.J. Welsh, Adenovirus fiber disrupts CAR-mediated intercellular adhesion allowing virus escape, *Cell* 110 (2002) 789–799.
- [10] R.P. Tomko, R. Xu, L. Philipson, HCAR and MCAR: the human and mouse cellular receptors for subgroup C adenoviruses and group B coxsackieviruses, *Proc. Natl. Acad. Sci. U. S. A.* 94 (1997) 3352–3356.
- [11] T. Chavakis, T. Keiper, R. Matz-Westphal, K. Hersemeyer, U.J. Sachs, P.P. Nawroth, K.T. Preissner, S. Santoso, The junctional adhesion molecule-C promotes neutrophil transendothelial migration *in vitro* and *in vivo*, *J. Biol. Chem.* 279 (2004) 55602–55608.
- [12] W. Ikeda, S. Kakunaga, K. Takekuni, T. Shingai, K. Satoh, K. Morimoto, M. Takeuchi, T. Imai, Y. Takai, Nectin-like molecule-5/Tage4 enhances cell migration in an integrin-dependent, nectin-3-independent manner, *J. Biol. Chem.* 279 (2004) 18015–18025.
- [13] L. Russell, Movement of spermatocytes from the basal to the adluminal compartment of the rat testis, *Am. J. Anat.* 148 (1977) 313–328.
- [14] C.Y. Cheng, D.D. Mruk, Cell junction dynamics in the testis: Sertoli–Germ cell interactions and male contraceptive development, *Physiol. Rev.* 82 (2002) 825–874.
- [15] L. Russell, Observations on rat Sertoli ectoplasmic (“junctional”) specializations in their association with germ cells of the rat testis, *Tissue Cell* 9 (1977) 475–498.
- [16] S. Mueller, T.A. Rosenquist, Y. Takai, R.A. Bronson, E. Wimmer, Loss of nectin-2 at Sertoli–spermatid junctions leads to male infertility and correlates with severe spermatozoan head and midpiece malformation, impaired binding to the zona pellucida, and oocyte penetration, *Biol. Reprod.* 69 (2003) 1330–1340.
- [17] G. Glikli, K. Ebnat, M. Aurrand-Lions, B.A. Imhof, R.H. Adams, Spermatid differentiation requires the assembly of a cell polarity complex downstream of junctional adhesion molecule-C, *Nature* 431 (2004) 320–324.
- [18] M. Mirza, J. Hreinsson, M.-L. Strand, O. Hovatta, O. Soder, L. Philipson, R.F. Pettersson, K. Sollerbrant, Coxsackievirus and adenovirus receptor (CAR) is expressed in male germ cells and forms a complex with the differentiation factor JAM-C in mouse testis, *Exp. Cell Res.* 312 (2006) 817–830.
- [19] I. Thoelen, C. Magnusson, S. Tagerud, C. Polacek, M. Lindberg, M. Van Ranst, Identification of alternative splice products encoded by the human coxsackie–adenovirus receptor gene, *Biochem. Biophys. Res. Commun.* 287 (2001) 216–222.
- [20] A. Dorner, D. Xiong, K. Couch, T. Yajima, K.U. Knowlton, Alternatively spliced soluble coxsackie–adenovirus receptors inhibit coxsackievirus infection, *J. Biol. Chem.* 279 (2004) 18497–18503.
- [21] J. Grima, L.-j. Zhu, C.Y. Cheng, Testin is tightly associated with testicular cell membrane upon its secretion by Sertoli cells whose steady-state mRNA level in the testis correlates with the turnover and integrity of inter-testicular cell junctions, *J. Biol. Chem.* 272 (1997) 6499–6509.
- [22] M. Galdieri, E. Ziparo, F. Palombi, M.A. Russo, M. Stefanini, Pure Sertoli cell cultures: a new model for the study of somatic–germ cell interactions, *J. Androl.* 2 (1981) 249–254.
- [23] M.K.Y. Siu, C.-h. Wong, W.M. Lee, C.Y. Cheng, Sertoli–germ cell anchoring junction dynamics in the testis are regulated by an interplay of lipid and protein kinases, *J. Biol. Chem.* 280 (2005) 25029–25047.
- [24] G.R. Aravindan, C.P. Pineau, C.W. Bardin, C.Y. Cheng, Ability of trypsin in mimicking germ cell factors that affect Sertoli cell secretory function, *J. Cell. Physiol.* 168 (1996) 123–133.
- [25] K. Zen, Y. Liu, I.C. McCall, T. Wu, W. Lee, B.A. Babbitt, A. Nusrat, C.A. Parkos, Neutrophil migration across tight junctions is mediated by adhesive interactions between epithelial coxsackie and adenovirus receptor and a junctional adhesion molecule-like protein on neutrophils, *Mol. Biol. Cell* 16 (2005) 2694–2703.
- [26] J. Grima, C.C.S. Wong, L.-j. Zhu, S.-d. Zong, C.Y. Cheng, Testin secreted by Sertoli cells is associated with the cell surface, and its expression correlates with the disruption of Sertoli–germ cell junctions but not the inter-Sertoli tight junction, *J. Biol. Chem.* 273 (1998) 21040–21053.
- [27] A.H.F.M. Peters, J. Drumm, C. Ferrell, D.A. Roth, D.M. Roth, M. McCaman, P.L. Novak, J. Friedman, R. Engler, R.E. Braun, Absence of germline infection in male mice following intraventricular injection of adenovirus, *Mol. Ther.* 4 (2001) 603–613.
- [28] M. Ito, M. Kodama, M. Masuko, M. Yamaura, K. Fuse, Y. Uesugi, S. Hirono, Y. Okura, K. Kato, Y. Hotta, T. Honda, R. Kuwano, Y. Aizawa, Expression of coxsackievirus and adenovirus receptor in hearts of rats with experimental autoimmune myocarditis, *Circ. Res.* 86 (2000) 275–280.
- [29] R.P. Tomko, C.B. Johansson, M. Totrov, R. Abagyan, J. Frisen, L. Philipson, Expression of the adenovirus receptor and its interaction with the fiber knob, *Exp. Cell Res.* 255 (2000) 47–55.
- [30] E.C. Roosen-Runge, In the Process of Spermatogenesis in Animals, Cambridge Univ. Press, Cambridge, U.K., 1977, pp. 1–12.
- [31] M.J. van Raaij, E. Chouin, H. van der Zandt, J.M. Bergelson, S. Cusack, Dimeric structure of the coxsackievirus and adenovirus receptor D1 domain at 1.7 Å resolution, *Structure* 8 (2000) 1147–1155.
- [32] M.C. Bewley, K. Springer, Y.-B. Zhang, P. Freimuth, J.M. Flanagan, Structural analysis of the mechanism of adenovirus binding to its human cellular receptor, CAR, *Science* 286 (1999) 1579–1583.
- [33] D.D. Mruk, C.Y. Cheng, Sertoli–Sertoli and Sertoli–germ cell interactions and their significance in germ cell movement in the seminiferous epithelium during spermatogenesis, *Endocr. Rev.* 25 (2004) 747–806.
- [34] C.B. Coyne, J.M. Bergelson, CAR: a virus receptor within the tight junction, *Adv. Drug Delivery Rev.* 57 (2005) 869–882.

- 961 [35] K. Ozaki-Kuroda, H. Nakanishi, H. Ohta, H. Tanaka, H. 997
 962 Kurihara, S. Mueller, K. Irie, W. Ikeda, T. Sakai, E. Wimmer, 998
 963 Nectin couples cell-cell adhesion and the actin scaffold at 999
 964 heterotypic testicular junctions, *Curr. Biol.* 12 (2002) 1000
 965 1145-1150. 1001
- 966 [36] M.D. Lacher, M.I. Tiirikainen, E.F. Saunier, C. Christian, M. 1002
 967 Anders, M. Oft, A. Balmain, R.J. Akhurst, W.M. Korn, 1003
 968 Transforming growth factor- β receptor inhibition enhances 1004
 969 adenoviral infectability of carcinoma cells via up-regulation 1005
 970 of coxsackie and adenovirus receptor in conjunction with 1006
 971 reversal of epithelial-mesenchymal transition, *Cancer Res.* 66 1007
 972 (2006) 1648-1657. 1008
- 973 [37] T. Vincent, R.F. Pettersson, R.G. Crystal, P.L. Leopold, 1009
 974 Cytokine-mediated downregulation of 1010
 975 coxsackievirus-adenovirus receptor in endothelial cells, 1011
 976 *J. Virol.* 78 (2004) 8047-8058. 1012
- 977 [38] A. Bruning, I.B. Runnebaum, CAR is a cell-cell adhesion 1013
 978 protein in human cancer cells and is expressionally 1014
 979 modulated by dexamethasone, TNF α and TGF β , *Gene Ther.* 10 1015
 980 (2003) 198-205. 1016
- 981 [39] A. Bruning, I.B. Runnebaum, The coxsackie adenovirus 1017
 982 receptor inhibits cancer cell migration, *Exp. Cell Res.* 298 1018
 983 (2004) 624-631. 1019
- 984 [40] M. Anders, C. Christian, M. McMahon, F. McCormick, W.M. 1020
 985 Korn, Inhibition of the Raf/MEK/ERK pathway up-regulates 1021
 986 expression of the coxsackievirus and adenovirus receptor in 1022
 987 cancer cells, *Cancer Res.* 63 (2003) 2088-2095. 1023
- 988 [41] M.K.Y. Siu, W.M. Lee, C.Y. Cheng, The interplay of collagen IV, 1024
 989 tumor necrosis factor- α , gelatinase B (matrix 1025
 990 metalloprotease-9), and tissue inhibitor of metalloproteases-1 1026
 991 in the basal lamina regulates Sertoli cell tight junction 1027
 992 dynamics in the rat testis, *Endocrinology* 144 (2003) 371-387. 1028
- 993 [42] S.K. De, H.L. Chen, J.L. Pace, J.S. Hunt, P.F. Terranova, G.C. 1029
 994 Enders, Expression of tumor necrosis factor- α in mouse 1030
 995 spermatogenic cells, *Endocrinology* 133 (1993) 389-396. 1031
- 996 [43] W.-y. Lui, W.M. Lee, C.Y. Cheng, Transforming growth factor 1032
 1033 b3 regulates the dynamics of Sertoli cell tight junctions via 997
 the p38 mitogen-activated protein kinase pathway, *Biol. 998
 Reprod.* 68 (2003) 1597-1612. 999
- [44] A. Persson, X. Fan, B. Widegren, E. Englund, Cell type- and 1000
 region-dependent coxsackie adenovirus receptor 1001
 expression in the central nervous system, *J. Neuro-Oncol.* 78 1002
 (2006) 1-6. 1003
- [45] W.-Y. Lui, C.-H. Wong, D.D. Mruk, C.Y. Cheng, TGF- β 3 1004
 regulates the blood-testis barrier dynamics via the p38 1005
 mitogen activated protein (MAP) kinase pathway: an *in vivo* 1006
 study, *Endocrinology* 144 (2003) 1139-1142. 1007
- [46] M.W.M. Li, W. Xia, D. Mruk, C.Q.F. Wang, H.H.N. Yan, M.K.Y. 1008
 Siu, W.-y. Lui, W.M. Lee, C.Y. Cheng, TNF α can reversibly 1009
 disrupt the blood-testis barrier (BTB) and impair Sertoli-germ 1010
 cell adhesion - a novel mechanism to regulate junction 1011
 dynamics during spermatogenesis, *J. Endocrinol.* 190 (2006) 1012
 315-331. 1013
- [47] R.W. Walters, T. Grunst, J.M. Bergelson, R.W. Finberg, M.J. 1014
 Welsh, J. Zabner, Basolateral localization of fiber receptors 1015
 limits adenovirus infection from the apical surface of airway 1016
 epithelia, *J. Biol. Chem.* 274 (1999) 10219-10226. 1017
- [48] C.J. Cohen, J. Gaetz, T. Ohman, J.M. Bergelson, Multiple regions 1018
 within the coxsackievirus and adenovirus receptor 1019
 cytoplasmic domain are required for basolateral sorting, 1020
J. Biol. Chem. 276 (2001) 25392-25398. 1021
- [49] C.-H. Wong, W. Xia, N.P.Y. Lee, D.D. Mruk, W.M. Lee, C.Y. 1022
 Cheng, Regulation of ectoplasmic specialization dynamics in 1023
 the seminiferous epithelium by focal adhesion-associated 1024
 proteins in testosterone-suppressed rat testes, *Endocrinology* 1025
 146 (2005) 1192-1204. 1026
- [50] C.B. Coyne, J.M. Bergelson, Virus-induced Abl and Fyn kinase 1027
 signals permit coxsackievirus entry through epithelial tight 1028
 junctions, *Cell* 124 (2006) 119-131. 1029
- [51] Y.-L. Chan, V. Paz, J. Olvera, I.G. Wool, The primary 1030
 structure of rat ribosomal protein S16, *FEBS Lett.* 263 (1990) 1031
 85-88. 1032